Slovak Biophysical Society

Institute of Molecular Physiology and Genetics SAS

IV. SLOVAK BIOPHYSICAL SYMPOSIUM

Modra-Harmonia

Slovakia

April 24 - 26, 2010

Scientific Committee

Karol Ondriaš (Institute of Mol. Physiol. & Gen. SAS, Bratislava)
Tibor Hianik (Faculty of Math., Physics and Inform. CU, Bratislava)
Pavol Balgavý (Faculty of Pharm. CU, Bratislava)

Organizing Committee

from Institute of Molecular Physiology & Genetics SAS, Bratislava

Marta Gaburjáková
Jana Gaburjáková
Andrej Rusnák
Andrej Opálek
Radoslav Janíček
Zuzana Tomášková
Barbora Tencerová
Andrea Faltinová

Sponsored by

H TEST a.s., Prague, Czech Republic
Agilent Technologies, Linz, Austria
Shimadzu Slovakia, Bratislava

TABLE OF CONTENTS

PROGRAM

SATURDAY, April 24, 2010

12.45 **Bus departure** from the parking place of Institute of Mol. Physiol. & Gen. SAS, Vlárska 5, Bratislava

14.00 - 15.30 **Registration** in Modra-Harmonia

14.00 - 18.00 **Poster installation**

15.30 - 15.45 **Opening ceremony**

15.45 - 16.45 **Session I.**
Molecular interactions, thermodynamics, spectroscopy
Chairs: D. Fedunová, P. Miškovský

15.45 - 16.00
O1 **G. Bánó**, J. Staničová, D. Jancura, J. Marek, M. Bánó, M. Savko, A. Dancáková, P. Miškovský: The diffusion of hypericin in DMSO/water mixtures

16.00 - 16.15
O2 **D. Búzová**, D. Jancura, P. Kasák, P. Miškovský: Solubilization of poorly soluble photosensitizer hypericin by polyethylen glycol

16.15 -16.30
O3 **D. Fedunová**, J. Bágeľová, Z. Gažová, M. Antalík: Prevention of thermal induced aggregation of proteins by complexation with polyanions

16.30 - 16.45
O4 **Ľ. Buriánková**, D. Jancura, Z. Naďová, M. Refregiers, J. Mikeš, P. Miškovský: Synchrotron based infrared microspectroscopy detection of apoptosis induced in human glioma cells by hypericin

16.45 - 17.00 **Coffee break**

17.00 - 18.00 **Session II.**
Molecular interactions, thermodynamics, spectroscopy
Chairs: Z. Gažová, Z. Tomášková

17.00 - 17.15
O5 **Z. Tomášková**, A. Špániková, S. Cacanyiová, P. Dočolomanský, K. Ondriaš: N-acetyl-L-cysteine interacts with NaHS induced release of NO

17.15 - 17.30

O6 A. Antošová, K. Šipošová, M. Koneracká, V. Závišová, P. Kopčanský, **Z. Gažová**: Lysozyme amyloid aggregates can be destroyed by magnetic fluids

17.30 - 18.00 **Plenary lecture**

P1 **I. Bernhardt**: Red blood cells: cell-cell and cell-surface interactions

18.30 **Welcome dinner**

SUNDAY, April 25, 2010

7.30 - 9.00 **Breakfast**

9.00 - 10.15 **Session III.**

Molecular interactions, thermodynamics, spectroscopy

Chairs: V. Huntošová, T. Hianik

9.00 - 9.15

O7 **T. Hianik**, A. Yu. Ryazanova, E. A. Kubareva, I. Grman, N. V. Lavrova, E. M. Ryazanova, T. S. Oretskaya: Application of surface acoustic method to study the interaction of proteins with nucleic acids

9.15 - 9.30

O8 **Z. Garaiová**, S. P. Strand, C. de Lange Davies: Internalization pathways of DNA-chitosan nanoparticles in Hela cells

9.30 - 9.45

O9 **P. Topor**, A. Mateašík, L. Bacharová: Visualization of mitochondria spatial distribution in living cells

9.45 - 10.00

O10 **V. Huntošová**, Z. Naďová, F. Sureau, P. Miškovský: Dynamics of hypericin redistribution in LDL and U87 glioma cells

10.00 – 10.15

O11 R. Kováč, I. Zahradník, **M. Novotová**: Ultrastructural changes in dyads of rat myocytes induced by a single dose of isoproterenol

10.15 - 10.45 **Coffee break**

10.45 - 12.30 **Session IV.**
Model and membrane systems
Chairs: J. Karlovská, T. Tokár

10.45 - 11.00
O12 **J. Karlovská**, P. Westh, P. Balgavý: DSC study of the thermal denaturation of Ca-ATPase reconstituted in phosphatidylcholine bilayers
11.00 - 11.15
O13 **M. Klacsová** , P. Westh, P. Balgavý: DSC study of the DMPC phase transition in presence of 1-alcohols
11.15 - 11.30
O14 **T. Tokár**, J. Uličný: Study of the ultrasensitivity of the Bcl-2 apoptotic switch
11.30 - 11.45
O15 C. Uličná, **J. Uličný**: Quantitative modeling of apoptosis – TNFR1 pathway
11.45 - 12.00
O16 **Ľ. Lacinová,** M. Karmažínová: Mechanism of gating of T-type calcium channels

12.00 - 12.30 **Business lecture**
B1 **G. Kada**, M. Duman, H.-P. Huber, I. Roth, Ch. Rankl, P. Hinterdorfer, F. Kienberger: A versatile toolset for nanometer scale research in life science

12.30 **Lunch**

14.00 - 15.45 **Session V.**
Membrane transport
Chairs: J. Gaburjáková, I. Zahradník

14.00 - 14.15
O17 **M. Gaburjáková**, J. Gaburjáková: Identification of changes in functional profile of the cardiac ryanodine receptor caused by the coupled gating phenomenon
14.15 - 14.30
O18 **J. Gaburjáková**, T. Kurucová, M. Gaburjáková: Modulation effect of caffeine on the activity of cardiac ryanodine receptor at physiological concentration of luminal Ca^{2+}
14.30 - 14.45
O19 **B. Tencerová**, M. Gaburjáková, A. Zahradníková: The effect of luminal Ca^{2+} on the cardiac ryanodine receptor in the presence of 2.5 mM ATP
14.45 - 15.00
O20 **A. Zahradníková**, I. Valent, I. Zahradník: Ryanodine receptor gating and activation of spontaneous calcium sparks

15.00 - 15.15
O21 **I. Zahradník**, I. Valent, A. Zahradníková: Recruitment of ryanodine receptor channels during calcium sparks
15.15 - 15.30
O22 **R. Janíček**, A. Zahradníková jr., E. Poláková, J. Pavelková, I. Zahradník, A. Zahradníková: Analysis of repetitive elementary calcium release events in rat cardiac myocytes
15.30 - 15.45
O23 **A. Zahradníková jr.**, E. Poláková, I. Zahradník, A. Zahradníková: Evidence for impaired local excitation-contraction coupling in isoproterenol-induced myocardial injury

15.45 - 16.00 **Coffee break**

16.00 - 17.00 **General Assembly of the Slovak Biophysical Society**

17.00 - 18.00 **Poster session**
Chairs: A. Zahradníková jr., K. Ondriaš

18.30 **Dinner**

MONDAY, April 26, 2010

7.30 - 9.00 **Breakfast**

9.00 – 10.00 **Session VI.**
Membrane channels, Molecular modeling and application of biophysics in medicine
Chairs: A. Zahradníková

9.00 - 9.15
O24 **L. Bryndzová**, V. Huntošová, J. Mikeš, Z. Naďová, F. Sureau, P. Miškovský: Intracellular distribution of hypericin (Hyp) and its effect on cell death
9.15 - 09.30
O25 **A. Rusnák**, L. Gibalová, Z. Sulová, A. Breier, B. Uhrík: Localization of cis-platinum in mouse neoplastic cells L1210

09.30 - 09.45
O26 **J. Suchánek**, I.K. Haverlík, G. Ruttkay-Nedecký: tRNA genes and the last universal common ancestor
09.45 - 10.00
O27 **K. Ondriaš**, Z. Tomášková, V. Komínková, Ľ. Máleková: Electrical properties of single mitochondrial channels

10.00 – 10.30 **Coffee break**

10.30 – 11.30 **Poster session**

11.30 **Concluding remarks**

12.00 **Lunch**

13:30 **Bus departure** to Bratislava

LIST OF ORAL PRESENTATIONS

PLENARY LECTURE

P1 **I. Bernhardt**: Red blood cells: cell-cell and cell-surface interactions

BUSINESS LECTURE

B1 **G. Kada**, M. Duman, H.-P. Huber, I. Roth, Ch. Rankl, P. Hinterdorfer, F. Kienberger: A versatile toolset for nanometer scale research in life science

SHORT ORAL PRESENTATIONS

O1 **G. Bánó**, J. Staničová, D. Jancura, J. Marek, M. Bánó, M. Savko, A. Dancáková, P. Miškovský: The diffusion of hypericin in DMSO/water mixtures

O2 **D. Búzová**, D. Jancura, P. Kasák, P. Miškovský: Solubilization of poorly soluble photosensitizer hypericin by polyethylen glycol

O3 **D. Fedunová**, J. Bágeľová, Z. Gažová, M. Antalík: Prevention of thermal induced aggregation of proteins by complexation with polyanions

O4 **Ľ. Buriánková**, D. Jancura, Z. Naďová, M. Refregiers, J. Mikeš, P. Miškovský: Synchrotron based infrared microspectroscopy detection of apoptosis induced in human glioma cells by hypericin

O5 **Z. Tomášková**, A. Špániková, S. Cacanyiová, P. Dočolomanský, K. Ondriaš: N-acetyl-L-cysteine interacts with NaHS induced release of NO

O6 A. Antošová, K. Šipošová, M. Koneracká, V. Závišová, P. Kopčanský, **Z. Gažová**: Lysozyme amyloid aggregates can be destroyed by magnetic fluid

O7 **T. Hianik**, A. Yu. Ryazanova, E. A. Kubareva, I. Grman, N. V. Lavrova, E. M. Ryazanova, T. S. Oretskaya: Application of surface acoustic method to study the interaction of proteins with nucleic acids

O8 **Z. Garaiová**, S. P. Strand, C. de Lange Davies: Internalization pathways of DNA-chitosan nanoparticles in Hela cells

O9 **P. Topor**, A. Mateašík, L. Bacharová: Visualization of mitochondria spatial distribution in living cells

O10 **V. Huntošová**, Z. Naďová, F. Sureau, P. Miškovský: Dynamics of hypericin redistribution in LDL and U87 glioma cells

O11 R. Kováč, I. Zahradník, **M. Novotová**: Ultrastructural changes in dyads of rat myocytes induced by a single dose of isoproterenol

O12 **J. Karlovská**, P. Westh, P. Balgavý: DSC study of the thermal denaturation of Ca-ATPase reconstituted in phosphatidylcholine bilayers

O13 **M. Klacsová**, P. Westh, P. Balgavý: DSC study of the DMPC phase transition in presence of 1-alcohols

O14 **T. Tokár**, J. Uličný: Study of the ultrasensitivity of the Bcl-2 apoptotic switch

O15 C. Uličná, **J. Uličný**: Quantitative modeling of apoptosis – TNFR1 pathway

O16 **Ľ. Lacinová**, M. Karmažínová: Mechnism of gating of T-type calcium channels

O17 **M. Gaburjáková**, J. Gaburjáková: Identification of changes in functional profile of the cardiac ryanodine receptor caused by the coupled gating phenomenon

O18 **J. Gaburjáková**, T. Kurucová, M. Gaburjáková: Modulation effect of caffeine on the activity of cardiac ryanodine receptor at physiological concentration of luminal Ca^{2+}

O19 **B. Tencerová**, M. Gaburjáková, A. Zahradníková: The effect of luminal Ca^{2+} on the cardiac ryanodine receptor in the presence of 2.5 mM ATP

O20 **A. Zahradníková**, I. Valent, I. Zahradník: Ryanodine receptor gating and activation of spontaneous calcium sparks

O21 **I. Zahradník**, I. Valent, A. Zahradníková: Recruitment of ryanodine receptor channels during calcium sparks

O22 **R. Janíček**, A. Zahradníková jr., E. Poláková, J. Pavelková, I. Zahradník, A. Zahradníková: Analysis of repetitive elementary calcium release events in rat cardiac myocytes

O23 **A. Zahradníková jr.**, E. Poláková, I. Zahradník, A. Zahradníková: Evidence for impaired local excitation-contraction coupling in isoproterenol-induced myocardial injury

O24 **L. Bryndzová**, V. Huntošová, J. Mikeš, Z. Naďová, F. Sureau, P. Miškovský: Intracellular distribution of hypericin (Hyp) and its effect on cell death

O25 **A. Rusnák**, L. Gibalová, Z. Sulová, A. Breier, B. Uhrík: Localization of cis-platinum in mouse neoplastic cells L1210

O26 **J. Suchánek**, I.K. Haverlík, G. Ruttkay-Nedecký: tRNA genes and the last universal common ancestor

O27 **K. Ondriaš**, Z. Tomášková, V. Komínková, Ľ. Máleková: Electrical properties of single mitochondrial channels

LIST OF POSTERS

P1 **A. Antošová**, K. Šipošová, E. Bystrenová, F. Valle, M. Koneracká, V. Závišová, P. Kopčanský, F. Biscarini, Z. Gažová: Magnetic fluid functionalized by albumin depolymerizes lysozyme amyloid fibrils

P2 **A. Faltinová**, J. Gaburjáková, Ľ. Urbániková, M. Hajduk, B. Tomášková, M. Antalík, A. Zahradníková: Effect of a domain peptide of the cardiac ryanodine receptor on the stability of the artificial lipid membrane

P3 **D. Fedunová**, Z. Flachbartová, J. Bágeľová, Z. Gažová, M. Antalík: Supramolecular complexes of α-lactalbumin with cytochrome c

P4 **J. Fischerová**, D. Chorvát: Spatial distribution and spectroscopic characterization of firefly luciferin in *Lampyris noctiluca*

P5 **J. Parnica**, L. Kandráč, M. Antalík: Influence of ionic liquids on conformation transitions of cytochrome c

P6 **M. Šimšíková**, M. Antalík: The study of optical properties of Mn-doped zinc oxide nanoparticles

P7 **K. Šipošová**, A. Antošová, P. Kutschy, Z. Daxnerová, Z. Gažová: Effect of phytoalexins on insulin amyloid aggregation

P8 L. Hubčík, **P. Pullmannová**, D. Uhríková, S. S. Funari, I. Lacko, F. Devínsky, P. Balgavý: Lipoplexes DNA – DOPC - gemini surfactant: a small angle X-ray diffraction and fluorescence spectroscopy

P9 **A. Krafčík**, P. Babinec: Theoretical analysis of motion of magnetic nanoparticles in high-gradient magnetic field: implications for cell separation, drug targeting and gene therapy

P10 **D. Kaljarová**, M. Babincová: Antioxidant properties of natural plant products: comparative analysis

BOOK OF ABSTRACTS

MAGNETIC FLUID FUNCTIONALIZED BY ALBUMIN DEPOLYMERIZES LYSOZYME AMYLOID FIBRILS

A. Antošová[1], K. Šipošová[2], E. Bystrenová[3], F. Valle[3], M. Koneracká[1], V. Závišová[1], P. Kopčanský[1], F. Biscarini[3], Z. Gažová[1]

[1]Department of Biophysics, Department of Magnetism, Institute of Experimental Physics SAS, Kosice, Slovakia, [2]Department of Biochemistry, Faculty of Science, P. J. Safarik University, Kosice, Slovakia, [3]Instituto per lo Studio dei Materiali Nanostrutturati ISMN-CNR, Bologna, Italy

Introduction: Protein self-assembly into amyloid aggregates is associated with a number of incurable human pathologies such as Alzheimer´s disease or type II diabetes [1]. Surprisingly, there are only few reports dealing with the effect of nanomaterials on amyloid aggregation. *In vitro* experiments indicate that some nanoparticles (NPs) (TiO_2, quantum dots) can accelerate fibril assembly kinetics. Contrary, disaggregation of lysozyme amyloid fibrils was observed for Fe_3O_4 nanoparticles [2]. The NPs able to reduced amyloid aggregation have great potential to be used as drugs to control amyloid diseases. We investigated ability of magnetic fluid functionalized by albumin to affect the amyloid fibrils formed by hen egg lysozyme as model amyloidogenic protein.

Material and Methods: The magnetic fluid functionalized by bovine serum albumin (MF-BSA) was prepared by co-precipitation of a mixture of salts of ferrous and ferric cations in alkaline medium. The obtained magnetic NPs were stabilized by sodium oleate to prevent their agglomeration. Adsorption of BSA was carried out by adding protein (10 % w/v solution) to the system under constant stirring at 50 °C and then left to cool down to room temperature. Lysozyme amyloid fibrils (LA) were obtained by incubation of protein (10μM) in presence of 80 mM NaCl, pH 2.7 under constant stirring at 65°C. The ability of MF-BSA to affect lysozyme amyloid aggregates *in vitro* was studied by ThT assay as the extent of amyloid aggregation is proportional to the fluorescence intensity of ThT. The morphology of the amyloid fibrils and aggregates was

investigated by AFM measurements performed by a stand-alone Smena NT-MDT microscope (PRA.MA. Sondalo, Italy) in semi-contact mode in air using silicon cantilevers NSG 11.

Result and Discussion: The properties of MF-BSA were characterized by different methods; typical AFM image of MF-BSA is in figure A. Incubation of the lysozyme amyloid fibrils (LA) (figure B) with MF-BSA caused decreasing of the ThT fluorescence indicating a reduction of the amount of amyloid aggregates. The extent of fibril disruption depends on MF-BSA concentration with extensive 90% reduction of amyloid aggregates for ratio LA:MF-BSA = 1:5. AFM measurements confirm the disaggregating effect of MF-BSA as it can be seen in figure C.

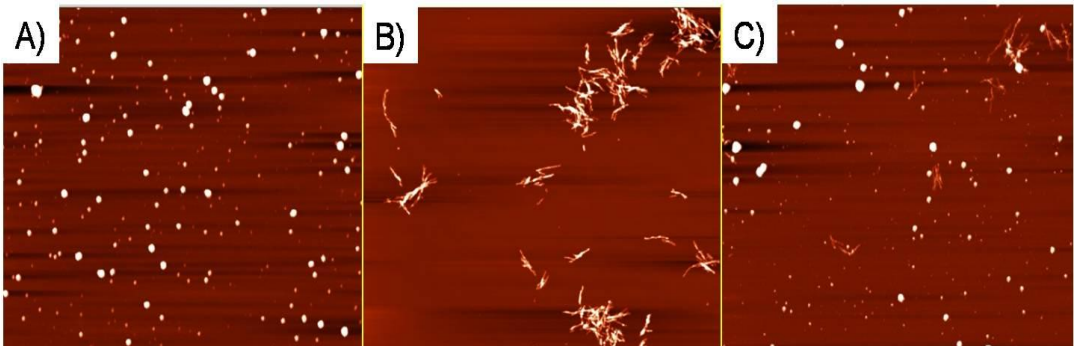

Figure: Typical AFM images of MF-BSA (10 μg/ml) (A), lysozyme amyloid fibrils (10 μg/ml) (B) and amyloid fibrils after overnight incubation with MF-BSA ratio LA : MF-BSA = 1: 1 (C).

Conclusion: The obtained results indicate that presence of MF-BSA led to disassembly of lysozyme amyloid aggregates. These features make MF-BSA of potential interest as therapeutic agents against amyloid-related diseases.

Acknowledgement

This work was supported within the projects Nos. 26220220005, 26220120033 in frame of SF EU, Project EU-NMP-STRP 032652 BIODOT, Centre of Excellence of SAS Nanofluid and VEGA 0079, 0056 and 0077.

References

[1] J. D. Sipe. *Amyloid proteins* (2005), Wiley-VCH, Weinheim and references inside.
[2] A. Bellova et al., *Nanotechnology* (2010) 21, 065103

THE DIFFUSION OF HYPERICIN IN DMSO/WATER MIXTURES

G. Bánó[1], J. Staničová[2], D. Jancura[1], J. Marek[3], M. Bánó[3], M. Savko[1], A. Dancáková[1], P. Miškovský[1]

[1]Biophysics Department, Šafárik University, Košice, Slovak Republic, [2]Institute of Biophysics and Biomathematics, UVMF, Košice, Slovak Republic, [3]Institute of Experimental Physics, SAV, Košice, Slovak Republic

Introduction: We report on diffusion coefficient of hypericin (Hyp) - a potential antiviral and anticancer agent [1] – in dimethylsulfoxide (DMSO)/water mixtures. It is our long-term aim to get a better insight into the diffusion phenomena of Hyp in solutions and across bio-membranes. Knowing of these processes is important for explanation of Hyp transport - as an agent in photodynamic therapy - into target tumor cells. Because of Hyp aggregation in aqueous environment its diffusion coefficient depends on the water content of the solvent. Falk et al [2] reported that with increasing water content a stacked aggregation of Hyp takes place in DMSO/water mixtures.

Material and methods: A modified diffusion-capillary method (Fig. 1) based on the measurement of absorbance changes was applied for diffusion coefficient measurements of Hyp.

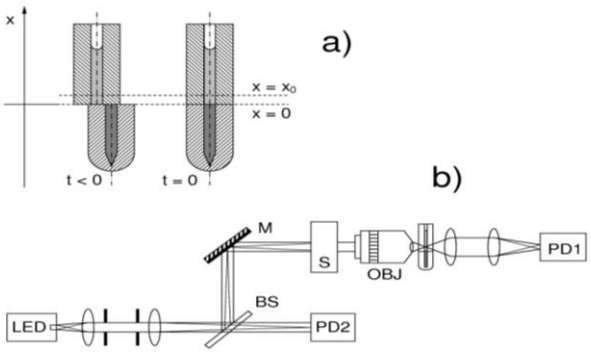

Fig. 1 The experimental setup for diffusion coefficient measurements. a) The two half capillaries - with and without the solute - before the measurements (misaligned) and at the beginning of the measurement at t = 0. b) The optical setup. PD1 and PD2 – photodiodes, BS – beam splitter, M – mirror, OBJ – microscope objective, S – shutter.

Results and discussion: The temporal dependence of Hyp absorbance is measured and fitted with the corresponding analytical solution of the one-dimensional diffusion equation (not shown). The effective diffusion coefficients (D_{eff}) of Hyp (at concentration of 10^{-4} M) obtained from these fits are plotted as a function of water percentage in DMSO/water mixtures (Fig. 2). Solid and dashed lines in Fig. 2 represent theoretical prediction (based on calculated friction coefficients) for the diffusion coefficient of different stacked Hyp aggregates. There is a good agreement of the experimental and calculated diffusion coefficient values of Hyp monomers in pure DMSO (Fig. 2). Our results indicate that Hyp stays in its monomeric (partially solvated) form up to 25 wt% of water in DMSO. Above 30 wt% of water Hyp starts to aggregate, which results in a gradually decreasing diffusion coefficient as compared to the diffusion coefficient of the monomeric form.

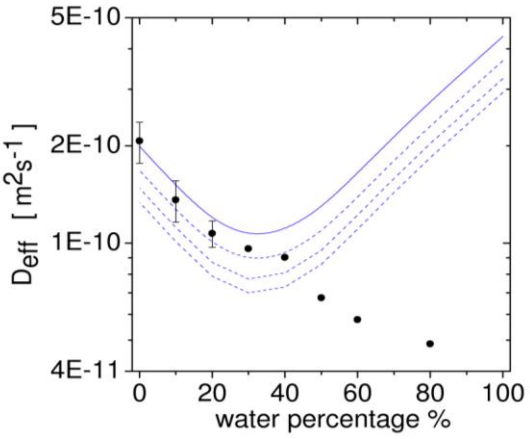

Fig. 2 Effective diffusion coefficients of Hyp as a function of water percentage in DMSO/water mixtures. Solid and dashed lines belong to calculated diffusion coefficient values of stacked Hyp aggregates containing 1 and 2 - 4 Hyp molecules, respectively.

Acknowledgements
This work was supported by the grant of Ministry of education VEGA No. 1/0124/08, KEGA No. 3/5115/07, LPP-0290-09, and APVV-0449-07.

References
[1] Lopez-Bazzochi, J.B. Hudson, G.H.N. Towers, *Photochem. Photobiol.* 54 (1991) 95-98.
[2] H. Falk, J. Mayer, *Monatsch Chem.* 125, (1994) 753-762.

RED BLOOD CELLS: CELL-CELL AND CELL-SURFACE INTERACTIONS

I. Bernhardt

Laboratory of Biophysics, Faculty 8, Saarland University, Saarbruecken, Germany

The lecture will focus on two subjects related to each other: cell-cell (1) and cell surface (2) interactions.

(1) Until recently, human red blood cells (RBCs) have been considered unable to undergo apoptosis since they lack mitochondria and nuclei. In addition, it is assumed that RBCs can play only a passive role in thrombus formation. However, recent investigations revealed that treatment of erythrocytes with Ca^{2+} and Ca^{2+} ionophore A23187 lead to cells shrinkage due to the efflux of KCl, and in addition to the exposure of phosphatidylserine (PS) on the outer leaflet of the cell membrane (measured by fluorescence microscopy and FACS on the basis of annexin-V binding), an indication of apoptosis. Both processes are related to (i) the activation of the Ca^{2+}-activated K^+ channel and (ii) the activation of the scramblase, due to an increase of the intracellular Ca^{2+} content. Our investigations focus on parameters like addition of prostaglandin E_2 and lysophosphatidic acid (both substances are released by thrombocytes after their activation) affecting the Ca^{2+} content and the PS exposure like A23187 treatment. To study whether the Ca^{2+} uptake of RBCs results in an enlargement of the mechanical cell-cell interaction, measurements applying holographic optical tweezers and AFM-based measurements of cell-cell adhesion forces have been carried out. It was possible to demonstrate that in the presence of Ca^{2+} and lysophosphatidic acid, attractive forces of about 200 pN were induced. Therefore, it seems possible to assume that RBCs play an active role in blood clot formation.

(2) RBCs from various mammalian species can have different resting shapes. Using the AFM technique, we demonstrate that a conformational change of integral membrane proteins can lead to an expansion of one leaflet of the membrane double layer relative to the other one and in turn results in a shape change. Such a protein-based expansion of one of the membrane leaflets is relatively fast. In addition, a very fast shape change can be observed when RBCs get in contact with a glass surface. To study the process of rapid shape changes of living (non-fixed) RBCs high resolution digital holographic microscopy has been applied. Using this method it is possible to perform time-resolved quantitative microscopic measurements of changes in the lateral and axial shape under different experimental conditions.

INTRACELLULAR DISTRIBUTION OF HYPERICIN AND ITS EFFECT ON CELL DEATH

L. Bryndzová[1], V. Huntošová[1,2], J. Mikeš[3], Z. Naďová[1], F. Sureau[2], P. Miškovský[1]

[1]Department of Biophysics UPJŠ, Kosice, Slovakia, [2]ANbioPhy CNRS UMR 7033, University Pierre and Marie Curie, Paris, France, [3] Institute of Biology and Ecology UPJŠ, Kosice, Slovakia

Introduction: Hypericin (Hyp) is a naturally occurring anthraquinone synthesized by plants of the genus *Hypericum* and is for its photosensitive properties very interested for photodynamic therapy (PDT) of cancer [1]. Photoactivated Hyp show antiproliferative and cytotoxic effects towards various cancerous cell-lines and is also suitable for initiation of apoptotic program in many cell cultures [2]. The key requirement for optimal response on photodynamic action is sufficient amount of photosensitizer inside cells. Hyp can be localized in different cells organelles. The occurrence of Hyp in different organelles depends mainly on used experimental protocol (concentration, incubation time) and cell line as well [2, 3, 4].

Material and Methods: Cells were seeded at $1x10^5$ cells/ 1 ml into cultivation flask for flow-cytometric assay or to Petri dish for fluorescence microscopy or FRET measurements. Cells were incubated 3 hours in 2 % Ultroser G medium with 500 nM Hyp as well in complex with LDL (20:1, 200:1) and then incubated with: LysoTracker Green DND-26, MitoTracker Green and $NBDC_6$-ceramide (fluorescent organelle markers).

Intracellular localization of Hyp was assessed by fluorescent microscopy. The experiments were performed on optiphot-2 epifluorescence microscope equipped with a Nipkow wheel coaxial-confocal attachment. The fluorescence lifetime value was calculated directly from either modulation or phase shift.

The number of living cells after photo-activation of Hyp was determined by MTT methods (% of survival cells). The type of cell death induced by Hyp photoactivation was assessed by flow cytometric analysis of Alexa Fluor®488 annexin V (Molecular Probes) and propidium iodide fluorescence.

Results and Discussion: Co-localization images showed that there is considerable localization of Hyp in perinuclear region. Significant fluorescent lifetime decrease was observed for NBDC6- ceramide (fluorescent probe for Golgi apparatus) in presence of 500 nM Hyp (≈2 ns). Significant differences in the proportional representation of live, apoptotic and/or necrotic cells were observed for different types of delivery systems of Hyp (Hyp vs. Hyp/LDL complexes) 24 hours after Hyp photoactivation.

Conclusion: Hyp is clearly localized in the Golgi apparatus. It can be concluded that subcellular localization depends on used delivery system and that the mode of cell death depends more on concentration of Hyp inside cells, than on different type of delivery systems.

Acknowledgement

This work was supported by the Slovak Research and Development Agency under contract APVV-0449-07, by scientific grant agency VEGA 1/0241/09 and by Slovak academic information agency.

References

[1] Miskovsky P., *Current Drug Targets*, 3 **(2002)**, 55-84.
[2] Agostini P., Vantiegehm A., Merlevede W., de Witte P. A. M., *Int. J. Biochem. Cell Biol.* 34 **(2002),** 221–241.
[3] Petrich J.W., *Int. Rev. Phys. Chem*. 19 **(2000)**, 479-500.
[4] Theodossiou T. A., Spiro M.D., Jacobson J., Hothersall J. S., Mac Robert A. J., *Photochem. Photobiol. Sci.*, 80 **(2004)**, 438-443.

SYNCHROTRON BASED INFRARED MICROSPECTROSCOPY DETECTION OF APOPTOSIS INDUCED IN HUMAN GLIOMA CELLS BY HYPERICIN

Ľ. Buriánková[1], D. Jancura[1], Z. Naďová[1], M. Refregiers[2], J. Mikeš[3], P. Miškovský[1,4]

[1]Department of Biophysics, Safarik University, Kosice, Slovakia, [2]Synchrotron SOLEIL, L'Orme des Merisiers, Saint-Aubin ,Gif sur Yvette, France,

[3]Institute of Biology and Ecology, Safarik University, Kosice, Slovakia,

[4]International Laser Center, Bratislava, Slovakia

Introduction: Hypericin (Hyp*)* is a natural photosensitizing pigment occurring in plants of the genus *Hypericum*, which under light illumination displays antiproliferative and cytotoxic effects on many tumor cells. By using synchrotron based Fourier transform infrared (SR-FTIR) microspectroscopy and flow-cytometry we investigated apoptotic death of U-87 MG cells induced by Hyp alone and in a complex with low-density lipoproteins (LDL).

Material and Methods:

Preparation of samples for SR-FTIR microspectroscopy experiments: U-87MG cell line was cultured on low-e slides in different cultivated media (10 % FBS, 2% UltroserG). UltroserG was used for an elevation of the number of LDL receptors on the cell surface. The cells were incubated for 3 hours in the medium with and without the presence of 500 nM Hyp and complexes Hyp/LDL (Hyp/LDL=30:1 and Hyp/LDL=200:1). The samples were then irradiated by light with wavelength 600 nm and the total irradiation dose was 4J/cm^2. 4 and 24 hours after irradiation the cells were washed with PBS (pH=7,2) and then they were incubated with 3,8% formalin for 20 minutes. After fixing with formalin, the cells were washed with water and let to be dried.

SR-FTIR microspectroscopy: The experiments were performed at Synchrotron SOLEIL (St Aubin, France) at the SMIS infrared beamline. The IR spectra were

collected in reflection mode using the IR Continuum XL microscope coupled to a ThermoNicolet 5700 microspectrometer. Each spectrum was acquired after 100 accumulation at spectral resolution 4cm^{-1}.

Results and Discussion: The differences between IR spectra of non-treated and Hyp treated cells are mainly manifested in the positions of Amide I and Amide II vibrational bands of proteins. These vibrational shifts are attributed to the protein structure changes from dominantly α-helix, in the non-treated cells, to β-sheets and random coil structures, which prevail 4h and 24h after photodynamic treatment, respectively. The observed conformational changes of proteins can be explained as the consequences of the processes leading to apoptosis. Flow cytometry experiments show only gently signs of apoptosis 4h after photodynamic treatment, the significant signs of apoptosis were observed after 24h. Both experimental approaches showed that the apoptosis in U-87 MG cells was induced more effectively by Hyp alone than in the presence of Hyp/LDL complexes.

Conclusion: The results confirm, that SR-FTIR microspectroscopy can be successfully applied for the detection of early apoptotic processes which are non-detectable by other experimental techniques.

Acknowledgement
This work was supported by the Slovak Research and Development Agency under contracts APVV-0449-07 and LPP-0337-06.

SOLUBILZATION OF POORLY SOLUBLE PHOTOSENSITIZER HYPERICIN BY POLYETHYLEN GLYCOL

D. Búzová[1], D. Jancura[1], P. Kasák[2], P. Miškovský[1,3]

[1]Department. of Biophysics, P.J. Safarik University, Kosice, Slovakia, [2]Polymer Institute SAV, Bratislava, Slovakia, [3]International Laser Center, Bratislava, Slovakia

Introduction: Hypericin (Hyp) is a promising agent for photodynamic therapy (PDT) of cancer and tumor diagnosis. Hyp under light illumination displays antiproliferative and cytotoxic effects on many tumor cell lines. Hyp is a lipophilic molecule and in aqueous environment forms insoluble aggregates. This makes intravenous injection of this drug problematic and restricts its medical applications. To overcome these problems, Hyp is usually incorporated into biological organisms by means of drug delivery systems (LDL, polyvinyl pyrrolidone, liposomes) which increase its solubility and bioavailability. One of the most popular drug carrier is polyethylen glycol (PEG). PEG is an uncharged hydrophilic polymer soluble in water composed of the simple repeating unit $HO\text{-}(CH_2\text{-}CH_2\text{-}O)_n\text{-}H$. For its biological aplications the following facts are the most inportant: the lack of immunogenicity, antigenicity and toxicity, high solubility in water and organic solvents, high flexibility of the chains and Food and Drug Administration (FDA) approval for human use. This work presents the results of the study of the influence of different types of PEG on solubilization of Hyp in aqueous solutions.

Material and Methods: By means of UV-VIS absorption and fluorescence spectroscopy we have studied the effect of length, molecular weight and concentration of PEG on the transition of aggregate form of Hyp to its monomeric form. Solutions for experiments were obtained by dilution of stock solutions of PEG and Hyp with phosphate buffer (pH=7,4) and were kept in the dark at room temperature for 2 hours before measurements. Absorption spectra of Hyp were measured on a UV-VIS spectrophotometer (SHIMADZU) in 200-

700 nm range. Fluorescence experiments were performed on fluorimeter SHIMADZU RF-301 with excitation at 550 nm and the intensity of fluorescence of Hyp was monitored at 599 nm.

Results: An increase of the intensity of Hyp fluorescence in the presence of PEG was observed. This increase is proportional to the molecular weight of molecules of PEG. With respect to the fact that the intensity of Hyp fluorescence corresponds to the amount of monomeric form of Hyp, we can conclude that PEG solubilize the aggregates of Hyp in aqueous solution. A similar study was realized for PEG/cholesterol and PEG/phospholipids (in this case PEG/phospholipids micelles are formed) conjugates. The intensity of Hyp fluorescence increases with the increase of conjugates concentration. We have also determined the dependence of absorption spectra of Hyp on PEG concentration for PEG molecules with different molecular weights (from 300 to 8000g.mol^{-1}). For PEG with low molecular weights (~ 300-600g.mol^{-1}), the absorption spectra of Hyp are similar to the absorption spectra of Hyp in aqueous solution and an increase of PEG concentration does not significantly changes character of these spectra. It signifies that low molecular PEG is not suitable for the monomerization of Hyp aggregates. PEG molecules with high molecular weights (>1000 g.mol^{-1}) are able to solubilize Hyp aggregates which is demonstrated by the absorption spectrum of Hyp in their presence similar to that for monomeric Hyp in organic solvents or lipids.

Conclusion: Length, molecular weight and concentration of PEG polymers affects a transition of Hyp from aggregate form to its monomeric form in aqueous solutions. PEG-cholesterol and PEG-phospholipids conjugates also solubilize Hyp aggregates in water. The results of this study contribute to the discussion about the searching of the "optimal" delivery system for hydrophobic/amphiphilic photosensitizers (e.g. Hyp).

Acknowledgements
This work was supported by the Slovak Research and Development Agency under contracts APVV-0449-07, LPP-0072-07 and the Scientific Grant Agency of the Ministry of Education of Slovak Republic (grant VEGA-0164-09).

EFFECT OF A DOMAIN PEPTIDE OF THE CARDIAC RYANODINE RECEPTOR ON THE STABILITY OF THE ARTIFICIAL LIPID MEMBRANE

A. Faltinová[1], J. Gaburjáková[1], Ľ. Urbániková[2], M. Hajduk[2], B. Tomášková[3], M. Antalík[3], A. Zahradníková[1]

[1]Institute of Molecular Physiology and Genetics SAS, Bratislava, Slovakia, [2]Institute of Molecular Biology SAS, Bratislava, Slovakia, [3]Institute of Experimental Physics SAS, Košice, Slovakia.

Introduction: Contraction of cardiac myocytes during the systole is induced by a transient elevation of cytosolic Ca^{2+} as a result of Ca^{2+} release from the intracellular stores through the Ca^{2+} release channel - ryanodine receptor (RyR2). RyR2 contains one N-terminal, one central and two C-terminal domains where mutations related to the cardiac arrhythmia, CPVT, tend to be clustered [1]. It is assumed that interaction between the N-terminal and the central domain plays a role in forming the "domain switch" that regulates the stability of the resting (closed) state of the RyR2 [2]. The aim of our study was to test this hypothesis for the N-terminal part of the RyR2. Our experimental strategy was based on the fact that the interaction between the examined RyR2 domains can be suppressed (i.e., channel can be activated) by adding a peptide with amino acid sequence identical to a part of the "domain switch" [3].

Material and Methods: We constructed the peptide DPcpvtN2 that corresponded to the N-terminal part of the RyR2 with the highest occurrence of CPVT mutations. The peptide was synthesized by GenScript Inc. (Piscataway, NJ, USA). We examined the effect of cytosolic DPcpvtN2 on the resting activity of rat RyR2 channels reconstituted into the artificial lipid membrane (BLM). Single-channel currents were recorded at a membrane potential of 0 mV under voltage-clamp conditions. For interpretation of our results we used bioinformatics methods, CD-spectroscopy and mapping on the known tertiary

structure of the IP3R ligand-binding domain [4] that is homologous with the distal part of the N-terminal domain.

Results and Discussion: We found that before an effect on the RyR2 activity could be observed, DPcpvtN2 interacted with the BLM. In the concentration range of 0.5 – 2.0 μM the peptide perforated the BLM regardless of the presence of the RyR2. Analysis of the secondary structure of DPcpvtN2 has shown a high incidence of α-helix (45 – 76 %). The hydrophobicity of DPcpvtN2 increases from the N-terminal to the C-terminal side. Such a gradient of hydrophobicity has been previously observed to cause insertion of small peptides at an angle of 30^o – 60^o at hydrophobic/hydrophilic interfaces, allowing the tilted peptides to perforate the lipid membrane [5]. These properties might explain the observed effect of DPcpvtN2 on the stability of BLM.

Conclusion: Our results indicate that is important to consider the effect of peptide ligands on the BLM, not only on the reconstituted channels.

Acknowledgements
This work was supported by the grants APVV-0139-06, APVV-0441-09, VEGA 02/0190/10 and by the European Union Contract No. LSHM-CT-2005-018833/EUGeneHeart.

References

[1] George CH et al.: *J. Mol. Cell Cardiol.* 42: 34-50, 2007.
[2] Yano M et al.: *Nat. Clin. Pract. Cardiovasc. Med.* 3: 43-52, 2006.
[3] Laver DR et al.: *Eur. Biophys. J.* 37: 455-67, 2008.
[4] Bosanac I et al.: *Nature* 420: 696-700, 2002.
[5] Brasseur R et al.: *Trends Biochem. Sci*. 22: 167-171, 1997.

SUPRAMOLECULAR COMPLEXES OF α-LACTALBUMIN WITH CYTOCHROME C

D. Fedunová[1], Z. Flachbartová[2], J. Bágeľová[1], Z. Gažová[1], M. Antalík[1,2]

[1]Institute of Experimental Physics SAS, Kosice, Slovakia, [2]Faculty of Science, University of P. J. Safarik, Kosice, Slovakia

Introduction: Targeted induction of apoptosis of pathological cells is one of the most challenging problems in medicine. Cytochrome c (cyt c) is an electron transport protein in respiratory chain, and it is also involved in the process of apoptosis after its release from mitochondria [1]. A new approach is oriented to the study of the ability of cyt c to induce apoptosis by its transport from extracellular location. One of the possible ways for its effective transport to the cell is the complexation with compounds facilitating this process [2].

In this work we have focused on study of interactions between α -lactalbumin (α-LA) and cyt c in order to find optimal conditions for their complexation. The main goal of this complexation is the further challenge of using these complexes in induction of programmed cell death.

Material and Methods: Absorption spectra were collected in a spectrophotometer Specord S 100 (Analytic Jena). Fluorescence intensity was measured by spectrofluorimeter Shimadzu RF-5000. Differential scanning calorimetry (DSC) measurements were carried out using the microcalorimeter DASM-4 with a heating rate of 1 °C/min. The experiments were performed in distilled water, 10 mM phosphate or cacodylate buffers, with or without presence of 2 mM $CaCl_2$ in pH range 2-11, cyt c concentration for spectroscopic measurements was 13μM and α-LA varied from 2,5 μM to 26 μM. For DSC measurement the protein concentration varied from 0.25 to 2 mg/ml.

Result and discussion: Presence of α-LA has caused no changes in absorption spectra of cyt c. In order to detect the cyt c – α-LA complex formation, we

examine the effect of α-LA on pKs of alkaline and acidic transition of cyt c. We have found that α-LA has only negligible effect on both pKs of cyt c. Slight increase of acidic pK of cyt c was observed in the presence of α-LA and oleic acid. The oleic acid stabilizes molten globular state of cyt c, which probably facilitates the interaction with cyt c. Although the presence of α-LA has not induced significant changes in heme pocket structure, interaction is manifested by turbidity increase even in low protein concentration. We have also observed the florescence quenching of inner tryptophan of α-LA in the presence of cyt c. From comparison with fluorescence quenching with free hemin follows that specific orientation of heme is needed for effective quenching provided by protein part during complexation. The complexation of cyt c with α-LA was also tested by calorimetric method. We have found that transition temperature of cyt c- α-LA complex at concentration ratio 1:1 and neutral pH is 65.2 ^{o}C, which is in the middle between transition temperatures of both free proteins (85.5 and 62.7 ^{o}C, resp.). It means that α-LA interacts with cyt c also at room temperature. The stability of the complex depends on protein concentration ratio and absolute concentration value.

Conclusion: α-LA has no signification effect on cyt c heme pocket structure within wide pH interval. The complex formation is manifested by turbidity increase even at low protein concentrations as well as from thermal stability changes. The properties of studied complexes depend on ionic strength.

Acknowledgement

This work was supported within the projects Nos. 26220220005, 2622022033 in frame of SF EU, Centre of Excellence of SAS Nanofluid and VEGA 0056, 0038 and 0079.

References

[1] Galluzzi, L., Zamzami, N., de La Motte Rouge, T., Lemaire, C., Brenner, C., Kroemer, G. (2007) *Apoptosis* **12**, 803-813.

[2] Duringer, C., Hamiche, A., Gustafsson, L., Kimura, H. Svanborg, C. (2003) *J Biol. Chem.* **278**, 42131-42135.

PREVENTION OF THERMAL INDUCED AGGREGATION OF PROTEINS BY COMPLEXATION WITH POLYANIONS

D. Fedunová[1], J. Bágeľová[1], Z. Gažová[1], M. Antalík[1,2]

[1]Institute of Experimental Physics SAS, Kosice, Slovakia, [2]Faculty of Science, University of P. J. Safarik, Kosice, Slovakia

Introduction: Protein aggregation frequently occurs *in vivo* as the symptoms of various diseases (prion, Alzhemier diseases, etc.) [1]. Additionally, treatment of proteins with stress conditions (heat, chemical denaturants) is accompanied by aggregation of denatured protein molecules during *in vitro* processing [2]. It is generally assumed that the major cause of aggregation is the insolubility of the denatured state. In an effort to understand the mechanisms of protein aggregation for medical as well as biotechnological purposes various test systems (aliphatic compounds, polyanions, denaturants) are used to counter hydrophobic interactions. We have studied the influence of two polyanions, poly(vinylsulfate) (PVS), and poly(4-styrene-sulfonate) (PSS) on cytochrome c (cyt c) aggregation at conditions near isoelectric pH, when strong aggregation occurs.

Material and Methods: The turbidity of the solutions was measured at 500 nm using SHIMADZU UV-3000 spectrophotometer with heating rate 1^{o}C/min. Differential scanning calorimetry (DSC) measurements were carried out using the microcalorimeter DASM-4 with a heating rate of 1 °C/min. The viscosity was measured by a Couette-type non-contact rotation viscometer [3] with shear rate of 60 s^{-1} and temperature scanning range from 15 to 80°C. Heating rate was 20 °C/h. The experiments were performed in 2 mM glycine buffer and 2 mM phosphate buffer, protein concentration was about 73 mM for DSC technique and viscometry, 7 mM for absorption spectroscopy. Polyanion concentration varied from 0.3 to 2 mg/ml.

Result and Discussion: At pH 10, very low reversibility of cyt c melting, very high reduced viscosity (60ml/g), and high turbidity indicate that cyt c forms aggregates in these conditions. Addition of PVS has led to the significant enhancement of thermal denaturation reversibility of this complex. The ability of PVS to increase the reversibility of cyt c transition depends on concentration. In the presence of unsaturated concentration of PVS, binding of several cyt c molecules to one polyanion chain has favored the aggregation of the protein. A large decrease in melting temperature of cyt c from 78.6 °C for free cyt c to 54.8 °C for cyt c - PVS complex at saturation concentration suggests the overall destabilization in protein tertiary structure. PSS has similar effect on cyt c denaturation only at low polyanion concentration. At higher concentration, PSS causes significant conformational change in hydrophobic core of protein as detected from disappearance of thermal transition. The stronger effect of PSS is attributed to the involvement of non-Coulombic interactions of the uncharged part of the polyanion molecule with the protein. In high ionic strength solutions, the interaction between PVS and cyt c disappears confirming the electrostatic character of protein–polyanion interaction.

Conclusion: Polyanions PVS and PSS enhance the thermal transition reversibility of cytochrome c in conditions near isoelectric pH by preventing the aggregation of denatured protein molecules probably due to steric hindrance as well as the repulsion between the charged groups of the polyanion chain and protein molecule. Data indicate that the polyanions are in complex with cytochrome c that is stabilized by synergistic effect of Coulombic and non-Coulombic interactions.

Acknowledgement
This work was supported within the projects Nos. 26220220005, 2622022033 in frame of SF EU, Centre of Excellence of SAS Nanofluid and VEGA 0056, 0038 and 0079.

References

[1] Shastry B., S. (2003) . *Neurochem Int.* **43**, 1–7.
[2] Weijers M, Barneveld P. A., Cohen Stuart M. A., Visschers R. W.(2003) *Protein Sci* **12**, 2693– 2703.
[3] Bano M., Strharsky I., Hrmo I.(2003) *Rev Sci Instrum* 74, 4788–4793.

SPATIAL DISTRIBUTION AND SPECTROSCOPIC CHARACTERIZATION OF FIREFLY LUCIFERIN IN *Lampyris noctiluca*

J. Fischerová [1], D. Chorvát [1,2,3]

[1]Department of Nuclear Physics and Biophysics, FMFI UK, Bratislava, Slovak Republic, [2]International Laser Centre, Bratislava, Slovak Republic, [3]Polymer Institute, SAV, Bratislava, Slovak Republic.

Introduction: Bioluminescence is the light emission in living organisms that appears as a result of specific chemical reactions. In Arthropoda the luminescence is due to catalytic reaction of luciferin with luciferase enzyme with the presence of ATP and oxygen. Luciferin, in addition to its bioluminescent character, is also fluorescent pigment, able to absorb UV light and emitting in blue-green spectral region, depending on its conformational state [1].

Material and Methods: Spatial distribution of Luciferin in *Lampyris noctiluca* was imaged either by custom fluorescence macro-imaging setup (Optem fiberoptic halogen source, Canon D-60 camera, glass filters) or using confocal laser scanning microscope (Zeiss LSM 510 META with 458nm Ar:ion excitation and 2.5x PlanNeofluar objective). For spectroscopic characterization of Luciferin (Invitrogen) we used absorption spectroscopy (Cary-50 Bio, Varian), fluorescence spectroscopy (Fluorolog 3-11, SPEX-Jobin/Yvon) and time-resolved spectroscopy (TCSPC setup from Becker-Hickl, Germany comprising of 375nm ps-pulsed diode laser, SPC-830 photon counting board and PML-SPEC multi-wavelength PMT array combined with Oriel spectrograph).

Results and Discussion: Fluorescence imaging of *Lampyris noctiluca* shows that the spatial distribution of fluorescence surprisingly does not completely collocalize with the location of its well-known luminescent organs (Fig.1.).

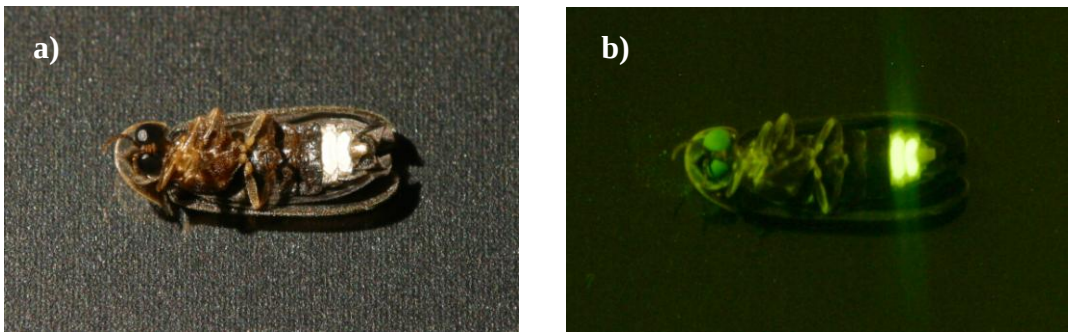

Figure 1.

Although the organs on the abdominal side show maximal fluorescence intensity, other parts such as eyes, legs or upper tectrices provide considerable amount of fluorescence signal as well. Following this observation we investigated fluorescence spectra at different locations of the firefly using multispectral confocal microscopy, and found no significant differences in the location of its spectral maximum. This result indicate that Luciferin is indeed the most likely dominant component responsible for the fluorescence of the animal.

To get deeper insight into luciferin spectroscopic properties we characterized the absorption and fluorescence spectra and the time-resolved fluorescence decays of purified Luciferin in solutions (water, ethanol and DMSO), as well as in solid phase (PMMA). The results were in accordance with previously published data, but surprisingly show that water environment is the only one that mimics the spectral behavior observed in the animal fluorescence (green emission around 500-550nm).

Conclusion: In this contribution we showed that spatial distribution of Luciferin fluorescence in *Lampyris noctiluca* is not constrained to its luminescent organs. Although more detailed spectroscopic characterization is needed to decipher its photophysical behaviour, fluorescence spectroscopy seems a promising tool for understand the evolutionary foundation of the firefly bioluminescent system [2].

References

[1] N.N. Ugarova and L.Y. Brovko, *Luminescence* 2002;17:321–330
[2] M. Dubuisson. C. Marchand and J-F. Rees, *Luminescence* 2004; 19: 339–344

tRNA GENES AND THE LAST UNIVERSAL COMMON ANCESTOR

J. S. Foltán[1], I. K. Haverlík[2], G. Ruttkay-Nedecký[2]

[1]Dept. of Informatics, Univ. of Trenčín, Slovak Republic, [2]Dept. of Nuclear Physics and Biophysics, FMFI UK, Bratislava, Slovak Republic

Introduction: Let a similarity between two sequences of *tRNA genes* be the number of sites that have the same nucleotide in the two sequences. Then a 1Mut-similarity $\overline{\mathrm{Sim}}^{gr}_{1\mathrm{Mut},\,S_i}$ is defined as the average similarity between such *tRNA genes* of a group of related organisms '*gr*' whose codons differ by one point mutation. 'S_i' specifies which sites of *tRNA genes* are included in computation. 1Mut-similarities were introduced and investigated in [1].

Material and Methods: Any aminoacyl-tRNA synthetase (aaRS) attaches a partial amino acid to a partial tRNA. An aaRS recognizes its tRNAs according to some of their nucleotides called *identity elements* (IE). Mutation of *major identity elements* leads to the strongest functional effects: S_{IE} are all IEs, S_{MIE} are major IEs mentioned at least 5 times and S_{MMIE} are the most major IEs mentioned at least 10 times in [2] for various aaRSs of various organisms. $S_{\mathrm{E.\ coli}}$ indicates IEs of *Escherichia coli*, while $S_{\mathrm{S.\ cer.}}$ are IEs of *Saccharomyces cerevisiae*. Let codons c_i and c_j differ by one point mutation and are assigned to sets $R_0^{gr}(c_r)$ and $R_0^{gr}(c_s)$ of tRNAs, respectively, in an alternative genetic code provided that $R_0^{gr}(c_r)$ and $R_0^{gr}(c_s)$ were assigned to c_r and c_s in the standard code GC_0. If c_r and c_s also differ by a point mutation, the pair c_i and c_j does not increase $\Delta_{\mathrm{bad\ 1Mut}}$. Otherwise, $\Delta_{\mathrm{bad\ 1Mut}}$ increases by 1. A total sum of such increments throughout all pairs of c_i and c_j gives the final value of $\Delta_{\mathrm{bad\ 1Mut}}$.

Results and Discussion: We developed a genetic algorithm to search a global maximum of 1Mut-similarities $\overline{\mathrm{Sim}}^{species}_{1\mathrm{Mut},\,S_i}$ over a set of $32! \approx 2.63 \times 10^{35}$ such alternative genetic codes in which assignments of the wobbling pairs of codons

affected by one tRNA were preserved or changed simultaneously. This global maximum is reached at the standard code for *tRNA genes* of no *archaeal* or *bacterial* species, but it is done 27 times for 4 sets of identity elements of *eukaryotic* species. In case of S_{MMIE} and S_{MIE}, it is also reached for average 1Mut-similarities among all single cell organisms and fungi (275 *cytoplasmic tRNA genes*), all animals (1344), all eukaryotes (1811) and even all organisms in our database (8163 *tRNA genes*) as well as all bacteria (5674 *tRNA genes*) in case of S_{MIE}. We used $\Delta_{\mathrm{bad\ 1Mut}}$ to measure a distance of a global maximum found by our algorithm from the standard code. The mean of these distances computed for *archaeal* species is 75.27 for S_{MMIE}, 69.82 for S_{MIE}, 82.55 for S_{IE} and 88.00 for S_{all}. The respective values among *bacterial* species are 83.36 (S_{MMIE}), 71.00 (S_{MIE}), 89.82 ($S_{\mathrm{E.\ coli}}$) and 82.45 (S_{all}), while they are 50.80 (S_{MMIE}), 8.00 (S_{MIE}), 12.80 ($S_{\mathrm{S.\ cer.}}$) and 11.20 (S_{all}) among *eukaryotic* species.

Conclusion: As seen global maxima of 1Mut-similarities $\overline{\mathrm{Sim}}^{species}_{1\mathrm{Mut},\,S_i}$ behave similarly for all the three domains of life, e.g., they all are best for S_{MIE}, but they are much closer to the standard genetic code in case of *eukaryotes*. In addition, $\Delta_{\mathrm{bad\ 1Mut}} = 0$ for $\overline{\mathrm{Sim}}^{all}_{1\mathrm{Mut},\,S_i}$ in case of both S_{MMIE} and S_{MIE}, which is some information about the common ancestor of all organisms. This supports a view that the last universal common ancestor (LUCA) was a protoeukaryote and *Archaea* and *Bacteria* have been products of reductive evolution.

References

[1] Foltan, J.S. tRNA genes and the genetic code. J. Theor. Biol. 2008, 253, 469-482.
[2] Giegé, R., Sissler, M., Florentz, C., 1998. Universal rules and idiosyncratic features in tRNA identity. Nucleic Acids Res. 26, 5017-5035.

MODULATION EFFECT OF CAFFEINE ON THE ACTIVITY OF CARDIAC RYANODINE RECEPTOR AT PHYSIOLOGICAL CONCENTRATION OF LUMINAL Ca^{2+}

J. Gaburjáková, T. Kurucová, M. Gaburjáková

Institute of Molecular Physiology and Genetics, Slovak Academy of Sciences, Vlarska 5, 833 34 Bratislava, Slovak Republic

Introduction: Ca^{2+} ions released from the sarcoplasmic reticulum *via* cardiac ryanodine receptor (RyR2) are the key determinant of cardiac contractility. The activity of RyR2 channel is primary controlled by Ca^{2+} entering the cytosol from the extracellular space through voltage-gated L-type Ca^{2+} channels. Recently, it has been shown that Ca^{2+} from the luminal face of the channel also regulates activity as well as gating kinetics of the RyR2 channel [1]. The aim of our present study was to investigate whether effects of luminal Ca^{2+} on the functional properties of the RyR2 observed at high concentration (53 mM) are also physiologically relevant. The amount of free Ca^{2+} in the lumen of the SR in cardiomyocytes was estimated to 1mM.

Material and Methods: The RyR2 channels were purified from rat heart and subsequently reconstituted into planar lipid bilayer. The cytosolic Ca^{2+} was kept at 90 nM concentration level and luminal side of the RyR2 channel complex was exposed to physiological concentration of luminal Ca^{2+} (1 mM). As a control - absence of luminal Ca^{2+} - we used Ba^{2+} ions. Under both experimental conditions we tested stimulation effect of caffeine added from the cytosolic side of the RyR2 channel. Observed results were compared with our previously published data obtained for 53 mM luminal Ca^{2+} [1].

Results and Discussion: We found that 1 mM luminal Ca^{2+} was similarly effective in enhancing the RyR2 channel sensitivity to caffeine and in decelerating the channel gating kinetics in comparison with control. Only one significant difference was identified between 1 mM and 53 mM luminal Ca^{2+}. 1 mM luminal Ca^{2+} decreased the maximal activation reached by the RyR2

channel by 2.5-fold (P_{omax} = 0,35 ± 0,14 for 1 mM luminal Ca^{2+} *vs.* P_{omax} = 0,87 ± 0,09 for 53 mM luminal Ca^{2+}).

Conclusion: Our results indicate that luminal Ca^{2+} interacts with potential Ca^{2+} binding sites localized on the luminal side of the RyR2 channel under physiological conditions and thus, the observed effects of luminal Ca^{2+} might play role in the regulation of RyR2 channel during the heart contraction.

Acknowledgement
This work was supported by the Slovak Grant Agency VEGA, project No. 2/0118/09.

References

[1] J. Gaburjakova, M. Gaburjakova: *J. Membr. Biol*. 212:17-28, 2006.

IDENTIFICATION OF CHANGES IN FUNCTIONAL PROFILE OF THE CARDIAC RYANODINE RECEPTOR CAUSED BY THE COUPLED GATING PHENOMENON

M. Gaburjáková, J. Gaburjáková

Institute of Molecular Physiology and Genetics, SAS, Bratislava, Slovak Republic

Introduction: In cardiac muscle, the intracellular trigger for contraction is a transient rise in intracellular free Ca^{2+} released from the Ca^{2+} stores through ryanodine receptor (RyR) channels. Two or more RyR channels reconstituted into a planar lipid membrane can open and close either independently (single gating) or simultaneously (coupled gating). Although the physiological relevance of coupled gating of RyR channels is largely open to debate at the present time, it has been considered as a one of termination mechanisms of Ca^{2+} release to ensure periodic contraction and relaxation of cardiac muscle [1]

Material and Methods: Cardiac microsomes isolated from the rat heart and enriched with RyR channels were incorporated into the planar lipid membrane and single channel currents were recorded under voltage-clamp conditions. As a charge carrier we used Ca^{2+} ions (5-53 mM) on the luminal face of RyR channels. The ion selectivity was determined in the presence of various mixtures of Ca^{2+} with Ba^{2+} ions while the total ion concentration was kept constant at 8 mM.

Results and Discussion: The objective of our work was to identify and further characterize potential changes in functional profile of the RyR channel caused by coupled gating phenomenon. We showed that coupled RyR channels isolated from the rat heart were activated by cytosolic Ca^{2+} with the similar efficacy and potency as was reported for the single RyR channel using the same experimental conditions. In contrast, all examined parameters of gating kinetics were affected by the functional interaction between channels. We first described the gating behavior of coupled RyR channels as a single functional unit, ignoring flicker

gating that likely reflects the thermodynamic stability of channel coupling and is the result of alternate brief transitions of individual RyR channels between open and closed states. In comparison with the single RyR channel, the average open and closed times were considerably prolonged and the frequency of opening was reduced. Interestingly, Ca^{2+} activated coupled RyR channels did not exhibit a sudden switch from slow to fast gating kinetics at open probability of 0.5 as was reported for the single RyR channel when luminal Ca^{2+} was used as a charge carrier. For flicker gating, the average closed time was significantly shorter and the frequency of closing was greatly enhanced. Furthermore, both parameters were independent on cytosolic Ca^{2+}, in contrary to the single RyR channel. Selected permeation properties of coupled RyR channels were comparable with those found for the single RyR channel. Ca^{2+} current amplitude - luminal Ca^{2+} relationship displayed a simple saturation and the channel selectivity for Ba^{2+} and Ca^{2+} ions was similar.

Conclusion: Our data suggest that the main purpose of a coupling between RyR channels is a synchronization of the channel gates to ensure mainly the correlation of Ca^{2+} fluxes, while the functional and the permeation properties of the individual RyR channels remain unchanged.

Acknowledgement
This work was supported by grant VEGA No. 2/0118/09.

References
[1] Stern M.D., Cheng H. (2004): Cell Calcium 35: 591-601

INTERNALIZATION PATHWAYS OF DNA-CHITOSAN NANOPARTICLES IN HELA CELLS

Z. Garaiová[1], S. P. Strand[2], C. de Lange Davies[2]

[1]Department of Nuclear Physics and Biophysics, FMFI UK, Bratislava, Slovak Republic, [2]Departments of Physics and Biotechnology, The Norwegian University of Science and Technology, Trondheim, Norway

Introduction: Chitosan is a natural, biodegradable cationic polymer that appears attractive as a non-viral vector for gene delivery. The cationic polysacharide chitosan interacts with DNA and forms nanoparticles also called polyplexes. Nonviral gene complexes can enter mammalian cells through different endocytic pathways. The contribution of certain pathways in the uptake of chitosan mediated gene delivery is not well understood and seems to be affected by cell type and the nature/characteristics of the gene carrier.

The purpose of our work was investigated the endocytic pathways involved in the uptake of chitosan/DNA nanoparticles.

Material and Methods: Two different chitosan (LIN, SB-TCO, 2mg/ml) with variable transfection efficiency have been studied. Plasmid DNA (g Wiz Luc, 0,5 mg/ml) was fluorescently labelled with the intercalating nucleic acid stain YOYO-1. These polyplexes are easily and efficiently internalized in Hela cells. Before studying the uptake of polyplexes, the Alexa-488 labelled transferrin–specific marker of clathrin-dependent endocytosis (CDE), has been used as positive control to find an optimal concentration of inhibitor. To study the involvement of CDE in polyplex uptake, cells were preincubated 30 min. before transfection with chlorpromazine or dynasore–specific inhibitors of CDE. The cells were incubated for 2 hours with chitosan/DNA-YOYO-1 nanoparticles and fluorescent endocytic probe transferrin. The cellular uptake of transferrin or DNA-chitosan polyplexes is analyzed by flow cytometry (Gallios).

Results and Discussion: As can been seen in Fig.1 cells were relatively insensitive to treatment with chlorpromazine at concetration 10 µg/ml.

A significant reduction in fluorescence intensity was observed in the presence of inhibitor at concentration 20 µg/ml.

The histograms show that all cells have taken up the polyplexes and the fluorescence intensity of the cells internalizing the polyplexes was approximately 80 times higher compared to the autofluorescence.

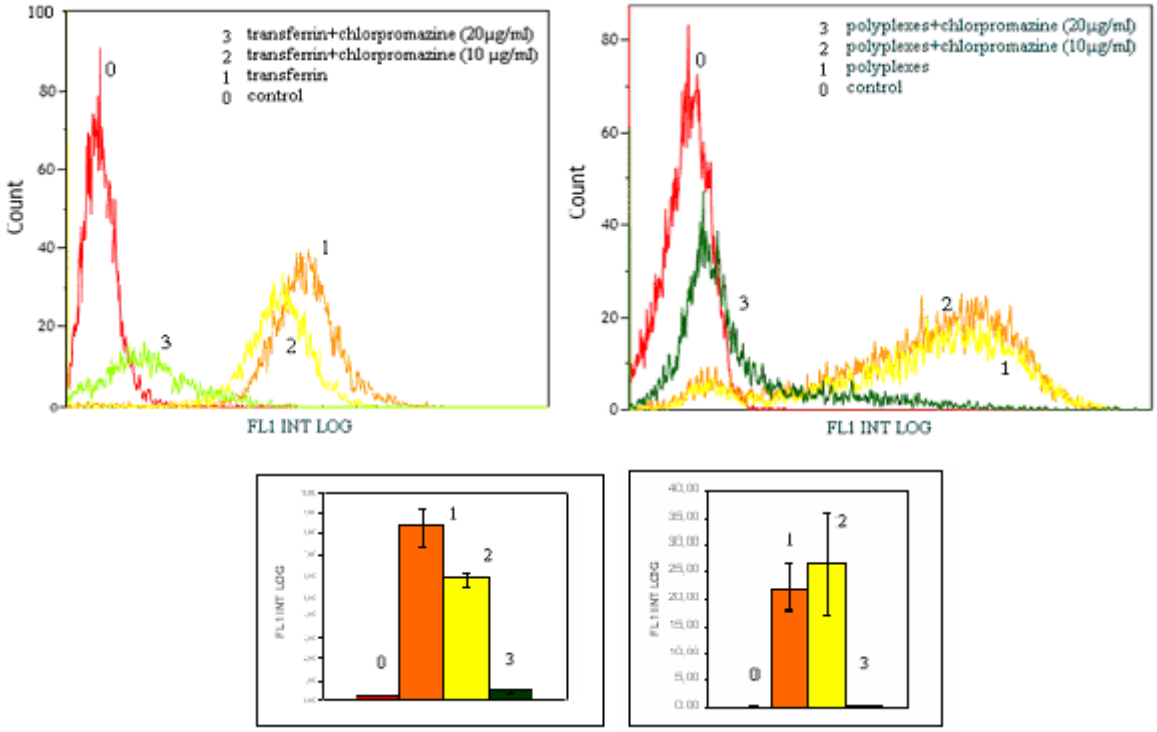

Fig.1: Cellular uptake of Alexa-488 labeled transferrin (left) and YOYO-1 labeled chitosan-DNA complexes (right) by the Hela cells treated with chlorpromazine. The graphs displays median ± SD fluorescence intensities of one of two independent experiments performed in triplicate. Control is an autofluorescence of non-treated cells. Per sample, 10 000 gated events were obtained.

Conclusion: Observations of this study indicate that internalization and transport of chitosan/DNA complexes in Hela cells follows clathrin-mediated endocytic pathway.

Acknowledgements

This work has been supported by EEA financial mechanisms, Norwegian financial mechanism and Slovak government by means of Fond NIL for promotion of collaboration in the field of education, Project No. NIL-I-006 and by Agency for Promotion Research and Development under the contract No. APVV-0250-09.

LYSOZYME AMYLOID AGGREGATES CAN BE DESTROYED BY MAGNETIC FLUIDS

A. Antošová[1], K. Šipošová[2], M. Koneracká[1], V. Závišová[1], P. Kopčanský[1], Z. Gažová[1]

[1]Department of Biophysics, Department of Magnetism, Institute of Experimental Physics SAS, Kosice, Slovakia, [2]Department of Biochemistry, Faculty of Science, P. J. Safarik Univerzity, Kosice, Slovakia

Introduction: Amyloidoses are protein misfolding disorders in which soluble proteins aggregate into insoluble fibrils, accumulation of which has been implicated in several diseases, such as Alzheimer's and Parkinson's diseases, or various forms of systemic amyloidosis [1]. Currently, there is no real cure available for treating the amyloid-related diseases. However, experimental data suggest that reduction of amyloid aggregates is beneficial. Interestingly, only a few studies are related to the effect of nanoparticles on amyloid aggregation of proteins. Recently we found that Fe_3O_4 magnetic nanoparticles are able to interact with lysozyme amyloids *in vitro* [3]. The obtained results initiated us to investigated effect of four magnetic fluids (MFs) on amyloid aggregation of hen egg white lysozyme as model amyloidogenic protein.

Material and Methods: Magnetic particles were synthesized by co-precipitation of ferric and ferrous salts in alkaline medium. Freshly prepared magnetic particles were dispersed in water (MF1, MF2, MF4) or physiological saline solution (MF3) and stabilized with perchloric acid (MF1) or sodium oleate (MF2, MF3, MF4). Bovine serum albumin (MF2) or dextran (MF4) was added as a modifying agent. Lysozyme amyloid aggregates were achieved by incubation of the protein (10μM) with 80 mM NaCl, pH 2.7 and constant stirring at 65°C.

Result and Discussion: Interaction of lysozyme amyloid aggregates (L_{agg}) with MFs was characterized by Thioflavin T fluorescence method (ThT assay) allowing quantification of the amount of protein in the state of amyloid aggregates.

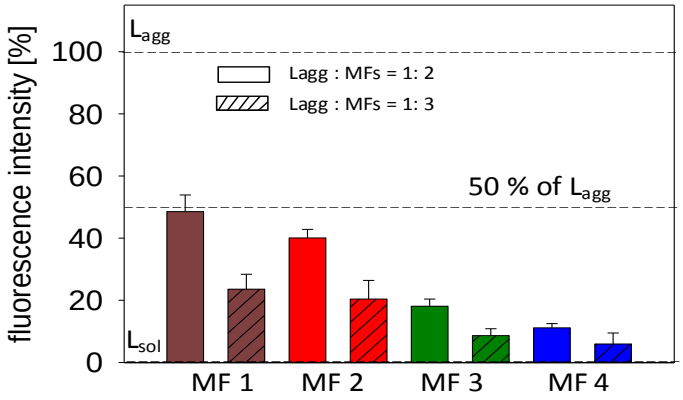

Figure: Extent of lysozyme amyloid aggregation in presence of magnetic fluid (MF1 - MF4) observed by ThT assay. Lysozyme amyloid aggregates (10 µM) were incubated with MF for 24 h in ratio L_{agg}:MF_{Fe3O4} = 1:2 and 1:3. Data were normalized to the fluorescence signal observed for lysozyme amyloid aggregates (L_{agg}) alone.

We have found that MFs are able to interact with amyloid fibrils *in vitro* resulting into decrease of the amount of lysozyme amyloid aggregates. Incubation of the amyloid fibrils with the studied MFs (at various w/w ratios of protein and magnetite component of MF_{Fe3O4}) led to significant reduction of amyloid aggregates: from 50 to 90 % detected for MF1 to MF4 for ratio L_{agg}:MF_{Fe3O4} = 1:2 and from 76% to 94% for ratio L_{agg}:MF_{Fe3O4} = 1:3. The depolymerizing effect of MFs was confirmed by electron microscopy.

Conclusion: The presence of all used magnetic fluids led to a disassembly of lysozyme amyloid aggregates. The extent of fibril disruption depended on the amount of added MF. Results suggest that anti-amyloid activity of MFs is significantly affected by composition of MFs. The MF4 containing dextran reduced the lysozyme amyloid aggregation most effectively. The obtained results make MFs of potential interest as therapeutic agents against amyloid-related diseases.

Acknowledgement
This work was supported within the projects Nos. 26220220005, 26220120033 in frame of SF EU, Centre of Excellence of SAS Nanofluid, and VEGA 0079, 0056, and 0077.

References:
[1] J. D. Sipe, *Amyloid proteins*, Wiley-VCH, Weinheim, (2005) and references inside.
[2] A. Bellova et. al., *Nanotechnology* (2010), 21, 065103.

APPLICATION OF SURFACE ACOUSTIC METHOD TO STUDY THE INTERACTION OF PROTEINS WITH NUCLEIC ACIDS

T. Hianik[1], A. Yu. Ryazanova[2], E. A. Kubareva[2], I. Grman[1], N. V. Lavrova[3], E. M. Ryazanova[4], T. S. Oretskaya[2]

[1]Department of Nuclear Physics and Biophysics, FMFI UK, Bratislava, Slovak Republic, [2]Faculty of Bioengineering and Bioinformatics, Chemistry Department, and Belozersky Institute of Physico-Chemical Biology, Lomonosov Moscow State University, Moscow, Russia, [3]Gamaleya Institute of Epidemiology and Microbiology, Moscow, Russia, [4]Institute of Agricultural Biotechnology, Moscow, Russia.

Introduction: The study of the mechanisms of protein–DNA interactions is of crucial importance for understanding the sequence-specific binding of proteins with natural DNA. Considering that typically 4–6 base pairs (bp) form a specific binding site for restriction enzymes, it is unlikely that the enzyme binds directly to this part of a long DNA. According to the current view, the protein binds initially non-specifically to the DNA and then moves to the specific site by various mechanisms, such as linear diffusion, jumping or intersegmental transfer [1]. In this work we have studied the interaction of (cytosine-5)-DNA methyltransferase SsoII (M.SsoII) with a model 60 bp DNA immobilized at the surface of a thickness shear mode quartz transducer (TSM). M.SsoII methylates cytosine residues at the methylation site in the presence of cofactor S-adenosyl-L-methionine. M.SsoII acts also as a transcription regulator when binding with the regulatory site. We have shown that the binding of M.SsoII to the DNA containing the specific sites is similar to those without specific sequences.

Materials and Methods: M.SsoII has been isolated according to Ref. [2]. Three types of 60 bp DNA duplexes containing the methylation site (60met), the regulatory site (60reg) or those without a specific site (60oct) were purchased from Thermo Fisher (Germany). One strand of each duplex has been modified by biotin, which allowed DNA immobilisation to the gold surface of the TSM

transducer covered by neutravidin (Pierce, USA). M.SsoII–DNA association has been studied by the TSM acoustic method [3].

Results and Discussion: Fig. 1 shows the changes of resonant frequency, Δf_s, as a function of protein concentration for the different TSM surface modifications. In the presence of M.SsoII similar frequency changes took place for the DNA studied, which suggests non-specific binding. It is likely to be caused by the electrostatic interactions. M.SsoII did not interact with neutravidin and no significant changes were observed for human serum albumin (HSA).

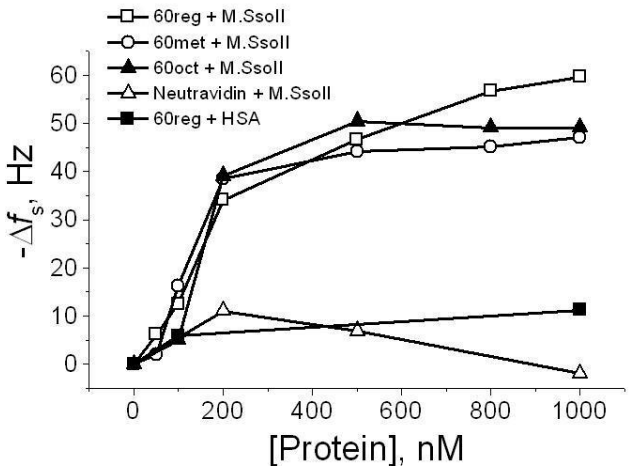

Fig. 1. The plot of the changes of resonance frequency as a function of protein concentration for the TSM transducers of different surface modification (see the legend).

Conclusion: It is likely that initially M.SsoII binds to DNA non- specifically. The dissociation constant K_d = 393±103 nM (60reg) has been similar for the interaction of M.SsoII with 60met and 60oct.

Acknowledgements
This work has been supported by Agency for Promotion Research and Development under the contract No. SK-RU-0010-07, by EÚ funded project Center of excellence for application of information macromolecules in prevention diseases and for improvement of the quality of life (Contract No. ITMS: 26240120003) and by Russian Foundation for Basic Research (grant No. 10-04-01578).

References

[1] S.E. Halford, Biochem. Soc. Trans. 37 (2009) 343.
[2] A.S. Karyagina *et al.*, Gene. 157 (1995) 93.
[3] T. Hianik *et al.*, Analyst 131 (2006) 1161.

DYNAMICS OF HYPERICIN REDISTRIBUTION IN LDL and U87 GLIOMA CELLS

V. Huntošová[1,2], Z. Naďová[1], F. Sureau[2], P. Miškovský[1]

[1]Department of Biophysics, UPJS, Kosice, Slovak Republic [2]ANBioPhy, CNRS FRE 3207 UPMC, Paris, France

Introduction: Cancer cells call for cholesterol to membrane construction during proliferation. Low-Density Lipoproteins (LDLs) are natural carriers of cholesterol in human body. Accordingly, human glioblastoma cell lines exhibit high levels of LDL-receptor and LDL-related proteins [Maletinska et al. 2000]. Hypericin (Hyp) is a highly hydrophobic molecule with a binding affinity of at least 20 Hyp molecules per 1 LDL molecule [Kascakova et al. 2005, Mukherjee et al. 2008]. For higher Hyp : LDL ratios (i.e. R> 20:1), aggregates formation started [Gbur et al. 2009, Huntosova et al. 2010]. Intracellular distribution of free Hyp is not specific, however when using LDL for vectorization, preferential localization in lysosomes could be achieved [Kascakova et al. 2008]. In our study redistribution of Hyp in cells by using Hyp saturated LDL (R> 20:1) are presented. In this condition, lost of the specificity for lysosomes and prefer membrane staining due to hydrophobic character of Hyp is observed.

Materials and Methods: U87-MG glioma cell line was used. Cells were grown in 2% Ultroser-G enriched D-MEM cultivation medium. Cellular uptakes of 500 nM Hyp either free in 1% DMSO or in complex with LDL were studied by Flow-cytometry. The 488 nm line of the Ar^+ laser was used for excitation and fluorescence was collected in FL3 channel (λ_{em}>590 nm). Further subcellular distributions of Hyp were obtained by epi-fluorescence microscopy in using a X63 water immersion objective (NA 1.2), excitation: 530-560 nm and emission >600 nm. Using Bodipy labeled LDLs (LDLb), Förster Resonance Energy Transfer (FRET) from the Bodipy fluorescent probe toward Hypericin was monitored by lifetime measurements in using a frequency domain fluorescence

lifetime micro-spectrometry (443 nm modulated excitation with frequencies ranging from 10 to 200MHz).

Results and Discussion: Cellular uptakes of free Hyp and Hyp-LDL complex refer to different time evolution of the fluorescence (see figure). Intracellular distribution is given by the corresponding fluorescence micro imaging. In the case of over loaded LDL (R=200:1) results are quite similar to those observed for Hyp alone. For lower concentration ratio (R=10:1) cellular uptake is decreased and the subcellular distribution shows a more specific localization in lysosome.

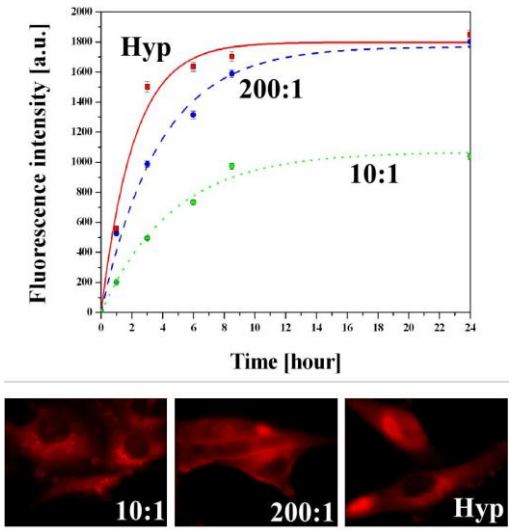

The Bodipy marker of LDLb in solution is characterized by a fluorescence lifetimes of 2.3 ns. After addition of 20 molecules of Hyp per LDL the fluorescence lifetime decreases to 1.1 ns due to the FRET from Bodipy toward Hyp.

For cells incubated either with free LDLb or with the complex [Hyp-LDLb] the intracellular fluorescence lifetime of Bodipy does not change (3.4 ns and 3.5 ns respectively) since Hyp is rapidly releases from the LDLb towards the cellular membrane.

Conclusion: LDL as natural carrier can effectively transport Hyp to cells, however when they are oversaturated, high losses of Hyp within blood flow could happened through rapid tredistribution toward other LDL or serum proteins molecules.

Acknowledgement
This project was supported by grants number: APVV-0449-07 and LPP-0337-06.

ANALYSIS OF REPETITIVE ELEMENTARY CALCIUM RELEASE EVENTS IN RAT CARDIAC MYOCYTES

R. Janíček, A. Zahradníková jr., E. Poláková, J. Pavelková, I. Zahradník, A. Zahradníková

Institute of Molecular Physiology and Genetics, SAV, Bratislava, Slovak Republic

Introduction: The main role of Ca^{2+} signaling in cardiac cells is to ensure the proper course and force of myocardial contraction. Both contraction and relaxation of myofibrils depend on the concentration of Ca^{2+} ions, which means that the time course and amplitude of the increase of Ca^{2+} concentration directly affect the time course and force of the contraction. After excitation of the cardiomyocyte, membrane Ca^{2+} current is activated and causes local calcium release from the sarcoplasmic reticulum *via* ryanodine receptors. The elementary events of calcium release can be observed by confocal microscopy as calcium spikes [1]. Stimulation usually causes a single spike at one release site, but occasionally two subsequent calcium spikes can be observed. These sequential release events are not sufficiently understood.

Material and Methods: We have studied the activation of calcium spikes by the calcium current in isolated rat ventricular myocytes. Calcium currents were activated by voltage pulses from -50 to 0 mV by means of the whole cell patch clamp method. The evoked local calcium release events/calcium spikes were recorded by confocal microscopy using the calcium indicator Fluo-3 (60 μM) in the presence of EGTA (1 mM) to limit Ca^{2+} diffusion [1], and analyzed by fitting with a theoretical function [2].

Results and Discussion: In the set of 30 recordings made in 18 myocytes, a large majority of the 305 observed calcium release sites responded to stimulation by a single calcium spike. In 13.4 % of observations the release sites responded by two subsequent (twin) spikes. The amplitude, latency, time to peak and duration of the single spikes were compared to those of the first and the

second of the twin spikes. Both the first and the second of the twin spikes had a lower amplitude than the single spikes. The sum of the amplitudes of the first and the second spikes was not significantly different from the amplitudes of single spikes.

On average, the second spikes had a shorter time to peak and a shorter duration than the first and the single spikes. The latency and the time to peak of the single and the first spikes were not significantly different. The mean interval between the first and the second spike was 21 ms. The incidence of twin spikes was higher when both the density and the inactivation rate of calcium current were reduced.

Conclusion: The analysis of the amplitudes of calcium spikes suggests that the twin calcium spikes occur at the same release site. The generation of the second spike may be a consequence of activation of a decreased number of ryanodine receptors in the calcium release unit during the first calcium spike. The shorter duration of the second spikes might be due to decreased luminal activation of the ryanodine receptors during the second spike after partial depletion of the sarcoplasmic reticulum cisterns. The distribution of calcium release into two parts may slow down the time course of both, the calcium release and the inactivation of calcium channels, and therefore it can affect both the shape of the action potential and the time course of the contraction.

Acknowledgement

Supported by grants APVV-0139-06 and VEGA 2/0102/08 and by the European Union Contract No. LSHM-CT-2005-018833/EUGeneHeart.

References

[1] Song LS et al.: *J Physiol (Lond)* 512: 677-691, 1998

[2] Zahradnikova A et al. *J Physiol (Lond).* 578: 677-691, 2007

A VERSATILE TOOLSET FOR NANOMETER SCALE RESEARCH IN LIFE SCIENCE

G. Kada[1], M. Duman[2], H.-P. Huber[2], I. Roth[2], Ch. Rankl[1], P. Hinterdorfer[2], F. Kienberger[1]

[1]Agilent Technologies, Nanomeasurements Division, Aubrunnerweg 11, 4040 Linz, Austria; [2]JKU University of Linz, Institute for Biophysics, Altenbergerstr. 69, 4040 Linz, Austria

This talk will focus on key Scanning Probe Microscopy (SPM) technology and introduce new and exciting developments for applications in the life sciences. Atomic Force Microscopy (AFM) has been widely used for imaging biological samples down to molecular and subunit resolution under physiological conditions. Moreover, a novel method has been developed for the localization of specific binding sites with nanometer positional accuracy by combining dynamic AFM with single molecule recognition force spectroscopy using functionalized tips, termed Topography and RECognition imaging (TREC).

In addition, optical imaging techniques enable the spectroscopic discrimination of different species in a biological sample. In particular, fluorescence microscopy has proven to be a powerful tool for selective and specific visualization of labeled molecules down to the single molecule level, rendering it possible to follow cellular processes and monitor the dynamics of living cell components. The advantages of AFM and fluorescence microscopy complement each other, and the combination of the two techniques allows a more detailed characterization of cellular structures and processes (Fig. 1-right).

The ultimate level of measuring structure and organization of membrane receptor proteins can be achieved by combining topography measurements with biological recognition mapping (using TREC) AND recording fluorescence images of the very same area (Fig. 1-left). A new way of designing an integrated

device which can combine seamlessly all three techniques into a single unit will be discussed.

This talk will finish with an introduction of a new technique, called near field Scanning Microwave Microscopy (SMM), with its potential of measuring changes in capacitance and dielectric constant of biological matter, thereby visualizing structures from underneath the surface.

References

[1] G. Kada, P. Hinterdorfer, F. Kienberger. Nanotoday 3 (2008), 12-19
[2] M. Duman et al, Nanotechnology 21 (2010), 115504

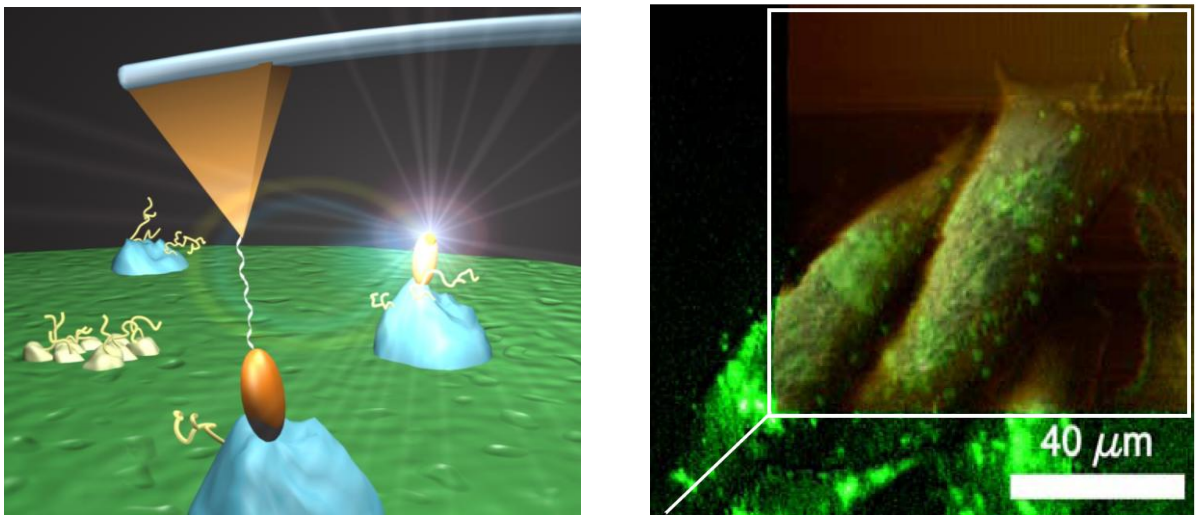

Figure 1 (left) Sketch of proteins in a cell membrane which can be detected by using (a) AFM topography imaging, (b) biological recognition imaging using a ligand on a string bound to the tip, and (c) fluorescence microscopy.

Figure 1 (right) Combined AFM/Fluorescence imaging of CHO cells (Chinese Hamster Ovary) expressing GFP-labeled cell receptors [2].

ANTIOXIDANT PROPERTIES OF NATURAL PLANT PRODUCTS: COMPARATIVE ANALYSIS

D. Kaljarová, M. Babincová

Department of Nuclear Physics and Biophysics, Faculty of Mathematics, Physics and Informatics, Comenius University, Mlynská dolina F1, 842 48 Bratislava 4, Slovak Republic

Introduction: Recently we have studied antioxidant activity of extract from *Scoparia dulcis* in oxidative process caused by UV radiation and Fenton reaction [1] as well as its gastroprotective effects [2]. In this work session we study antioxidant activities of some natural products by using a system of unilamellar liposomes. Peroxidative process was initiated by α,α´-Azodiisobutyramidine dihydrochloride (AAPH) which produces free radicals damaging lipid bilayer membrane. We studied antioxidant activity natural products as *Scoparia dulcis* and species of *Camellia sinensis*. *Scoparia dulcis* is a weed widespread in Laos and Vietnam and it is widely used by indigenous people to reduced aches, pain, fever, and for detoxication organism. Longevity tea (black), Te Guanyin (oolong) tea, Special Chun Mee tea (green) and Pai Mu Tan Superior (white) are species of plant *Camellia sinensis* whose leaves and leaf buds are used to produce tea for almost 5000 years [3]. In summary, we have compared antioxidant activities of natural products with well-known antioxidant α- tocopherol (vitamine E).

Material and Methods: Liposomes from phosphatidylcholine were prepared by Bangham hydratation method and consequently sonicated (Brown Labsonic). Lipid peroxidation was monitored by measurement of absorbtion spectra in the wavelength range 215- 233 nm using UV-VIS spectrophotometer (UVmini-1240 Shimadzu). The increase of the absorbtion at 233 nm was considered as evidence of formation of conjugated dienes. Klein oxidation index was calculated from the ratio of the absorbances $I = A_{233}/A_{215}$ [4].

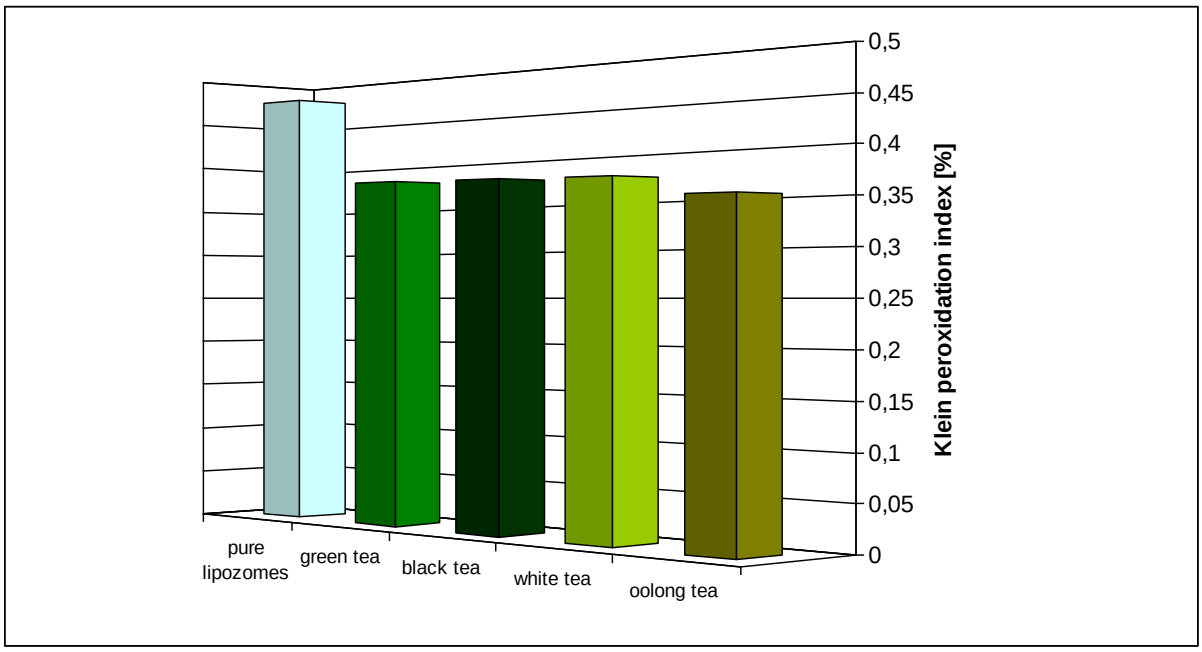

Fig.1. Influence of four different tea extracts on lipid peroxidation.

Results and Discussion: We studied peroxidation of liposomes initiated by AAPH reagent. Antioxidant activity of natural products was monitored by encapsulating them in a different concentration into structure of liposomes and measuring changes of peroxidation index with concentration of extracts from *Scoparia dulcis* and four species of tea-plant *Camellia sinensis*. Obtained results imply that *Scoparia dulcis* compared with α-tocopherol is an equally efficient scavenger of AAPH radicals and antioxidant activity of *Camellia sinensis* decrease in a sequence (Fig.1): oolong tea > white tea > black tea > green tea.

References

[1] Sourivong, P., Schronerova, K., Babincova, M. Scoparone inhibits ultraviolet radiation-induced lipid peroxidation. *Z. Naturforsch*. **62c** (2007) 61.
[2] Babincova, M., Schronerova, K., Sourivong, P. Antiulcer of water extract of Scoparia dulcis. *Fitoterapia* **79** (2009) 587.
[3] Sharangi, A.B. Medicinal and therapeutic potentialities of tea (Camelia sinensis L.). *Food Research International* **42** (2009) 529.
[4] Klein RA. The detection of oxidation in liposome preparation. *Biochem. Biophys. Acta* **210** (1970) 486.

DSC STUDY OF THE THERMAL DENATURATION OF Ca-ATPASE RECONSTITUTED IN PHOSPHATIDYLCHOLINE BILAYERS

J. Karlovská[1], P. Westh[2], P. Balgavý[1]

[1]Faculty of Pharmacy, Comenius University, Bratislava, Slovakia, [2]Department of Life Sciences and Chemistry, Roskilde University, Roskilde, Denmark

Introduction: Properties of ion transporting (Ca^{2+}-Mg^{2+}) ATPase from skeletal muscle sarcoplasmic reticulum (Ca-ATPase, EC 3.6.1.38) are dependent on its interactions with lipids surrounding it in bilayers [1,2]. In the present communication we study its thermal stability when reconstituted into lipid vesicles from 1,2-diacylphosphatidylcholines with monounsaturated acyl chains (diCn:1PC, n is the number of acyl carbons), using a differential scanning calorimetry (DSC).

Material and Methods: The synthetic diCn:1PCs were purchased from Avanti Polar Lipids (Alabaster, USA). The Ca-ATPase was isolated from the rabbit white muscle sarcoplasmic reticulum, purified and reconstituted as described in [2]. DSC experiments were performed on nano-DSC III CSC 6300 (TA Instruments, USA), at a scanning rate 0.6 °C/min. From the thermograms corrected for baselines, the transition temperature t_m and the calorimetric enthalpy ΔH_{cal} were determined.

Results and Discussion: The denaturation temperature of reconstituted Ca-ATPase varied between 47 and 52^{o}C, depending on the diCn:1PC acyl chain length, with a maximum for diC18:1PC at t_m=51.71^{o}C. The calorimetric enthalpy, which characterises the quantity of heat that is used for the protein denaturation, changed between 726 and 1055 kJ/(mol of Ca-ATPase) with a maximum for di(C18:1)PC. Elongation or shortening of diCn:1PC acyl chains surrounding the Ca-ATPase leads to decrease of both t_m and ΔH_{cal}. The Ca-ATPase is most stable in diC18:1PC bilayers and this correlates well with its activity [2].

Conclusion: The thermal stability of Ca-ATPase reconstituted in bilayers from monounsaturated phosphatidylcholines is sensitive to their acyl chain length with a maximum for dioleoylphosphatidylcholine.

Acknowledgements
This work was supported by the VEGA 1/0295/08 grant and JINR 07-4-1069-09/2011 project.

References
[1] Lee AG (2002) Biochim. Biophys. Acta 1565, 246-266
[2] Karlovská J, Uhríková D, Kučerka N, Teixeira J, Devínsky F, Lacko I, Balgavý P (2006) Biophys. Chem. 119, 69-77

DSC STUDY OF THE DMPC PHASE TRANSITION IN PRESENCE OF 1-ALCOHOLS

M. Klacsová[1,2], P. Westh[3], P. Balgavý[2]

[1]Faculty of Mathematics, Physics and Informatics and [2]Faculty of Pharmacy, Comenius University, Bratislava, Slovakia, [3]Department of Life Sciences and Chemistry, Roskilde University, Roskilde, Denmark

Introduction: Lee [1] and Trudell [2] proposed that alcohols may alter the equilibrium between highly ordered lipids in the solid-like bilayers and disordered lipids in the fluid bilayers. In their model, lipids surrounding a protein – ion channel need to be in more compressible fluid state in order for the ion channel to open. Alcohols would thus depress ion channel function by decreasing the temperature at which the lipids enter the solid-like state. Such ion channels are distributed along the membrane in non-myelinated and localized at the Ranvier nodes in myelinated nerves. During the lipid melting the heat capacity, volume and area compressibilities, all reach maxima [3]. Heimburg and Jackson therefore proposed a new model of nerve pulse propagation [3]. In the soliton model, nerve pulse forces the membrane through the phase transition from fluid to solid-like state. As anesthetic alcohols lower the phase transition temperature [1], it becomes more difficult to force the membrane through this transition and the generation of action potential is therefore suppressed. In present communication we report our results of effects of 1-alcohols (CnOH, n = 8 – 18 is the even number of alkyl carbons) on dimyristoylphosphatidyl-choline (DMPC) bilayers phase transitions using differential scanning calorimetry (DSC).

Material and Methods: DMPC was purchased from Avanti Polar Lipids (Alabaster, USA) and CnOHs from Sigma (St. Louis, USA). Samples were hydrated with redistilled water to 0.5 w% lipid concentration. DSC experiments were performed on nano-DSC III CSC 6300 (TA Instruments, USA). A dispersion of lipid was heated at a constant rate 1 °C/min. The transition

temperature was defined as the temperature where the dependence of specific heat capacity $C_p=f(t)$ reaches its maximum and was found by fitting the data with Pearson function. The calorimetric enthalpy ΔH_{cal} of the phase transition was determined as the total integrated area under the thermogram peak and the melting entropy was calculated using equation $\Delta S = \Delta H_{cal}/T_m$.

Results and Discussion: The melting temperature of pure DMPC was $t_m \sim 23.7$ °C. C10OH showed a biphasic effect on t_m, in accordance with literature. However, C12OH was found to monotonously increase t_m in the whole concentration range studied. At anesthetically relevant concentrations, C8OH and C10OH, which are known as anesthetically active alcohols, decreased t_m of DMPC. Longer alcohols which do not exhibit anesthetic action, increased it. The enthalpy ΔH and entropy ΔS change of the DMPC main transition corresponded to 31.3 kJ/mol and 105 J/mol.K, respectively. In the DMPC+C10OH system ΔH as well as ΔS showed a nonlinear increasing tendency with a breakpoint at C10OH:DMPC=0.4 mol/mol ratio. This breakpoint suggests increased ordering and alterations of interlipid interactions due to formation of a new phase at higher mole ratios. In the DMPC+C12OH system ΔH and ΔS increased monotonously with the C12OH concentration. In presence of C14OH (at C14OH:DMPC=0.2 mol/mol) these parameters reached a maximum. With further increase of CnOH chain length the enthalpy and entropy changes decreased. This effect may account for enhanced lipid-alcohol interactions at longer CnOHs, leading to increased ordering of the lipid bilayer.

Conclusion: Our results support the thermodynamical model of nerve pulse propagation and anesthetic action proposed by Heimburg and Jackson [3].

Acknowledgements
This work was supported by the VEGA 1/0295/08 grant and JINR 07-4-1069-09/2011 project.

References

[1] Lee AG (1976) Biochemistry 15, 2448-54
[2] Trudell JR (1977) Anesthesiology 46, 5-10
[3] Heimburg T, Jackson AD (2005) Proc Natl Acad Sci USA 102, 9790-95

THEORETICAL ANALYSIS OF MOTION OF MAGNETIC NANOPARTICLES IN HIGH-GRADIENT MAGNETIC FIELD: IMPLICATIONS FOR CELL SEPARATION, DRUG TARGETING AND GENE THERAPY

A. Krafčík, P. Babinec

Department of Nuclear Physics and Biophysics, Faculty of Mathematics, Physics and Informatics, Comenius University, Bratislava, Slovak Republic

The magnetic nanoparticles (MNPs) play a crucial role as drug carriers in the human body [1]. Their combination with strongly non-homogeneous magnetic field is considered as a useful way to focus MNPs functionalized with various drugs or genes to desired sites in living organism. Moreover superparamagnetic nanoparticles together with magnetic microparticles can be used as cell and molecules sorters for *in vitro* applications, or magnetofection. According to possible biomedical applications it is interesting to theoretically study behavior of mentioned particles moving in viscous fluid medium in presence of magnetic field source with high gradient flux density. The forces acting on magnetic particles are of different origins. The strongest forces affecting the motion are magnetic force and Stokes' viscous drag force [2]. Influence of several other interactions, like thermal kinetics, particle fluid interactions and interparticle effects e.g. magnetic dipole interactions, electric double layer interactions, and van der Waals; and inertia, buoyancy and gravity force are negligible.

We have considered motion of magnetic particles (magnetite, density 5000 $kg.m^{-3}$, saturation magnetization = 4.78×10^{5} $A.m^{-1}$) with radius 50 nm to 10 μm in several sources of magnetic field like cylindrical Halbach array of permanent magnets NdFeB N37, originally homogenous magnetic field (HMF, B = 0.46T) affected by micrometric ferromagnetic dots (supermalloy, radius = 5 μm), and also coil (inner diameter = 4 cm, 1000 turns, pulsed current = 1000 A). The Finite Element Method (FEMM v4.2, David Meeker) is applied to solve

Maxwell equations describing electromagnetic field. Motion of magnetic particles driven by magnetic force and affected by drag forces of viscous ambient (water, air) in a given magnetic field is obtained by solving set of ordinary differential equations expressed by Newton law of motion using numerical solver *ode23s* of Matlab 7.0 (The MathWorks).

Parameters like mean capture time, reach radius or motion velocity of magnetic particles have shown that studied systems are potentially applicable for magnetic cell/molecule separators, gene magnetofection or gene gun. Observed parameters can be significantly induced by interparticle interactions, which are responsible for agglomeration of nanoparticles utilized as carriers of bonded molecules, genes, etc, and which could be the object of further investigation.

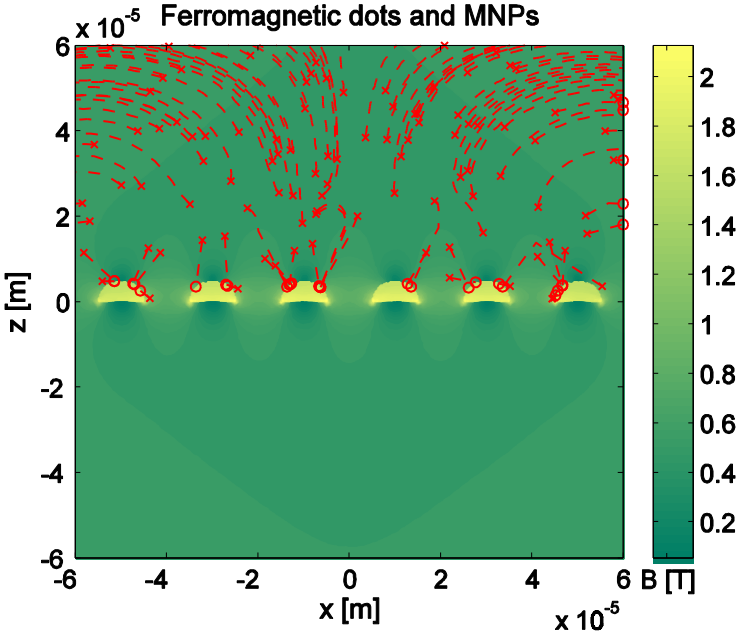

Figure 1 Trajectory of magnetite MNPs (diameter 100nm) in HMF (B = 0.46T) affected by supermalloy dots. Effective reach radius is approximately 20 μm.

References

[1] M. Babincova, V. Altanerova, C. Altaner, C. Bergemann, and P. Babinec, IEEE Transactions on Nanobioscience, 7, pp. 15-19, (2008).

[2] A. Krafčík, M. Babincová, and P. Babinec, Optoelectronics and Advanced Materials – Rapid Communications, 3, pp. 226-233, (2009).

GATING OF THE T-TYPE CALCIUM CHANNELS

Ľ. Lacinová, M. Karmažínová

Institute of Molecular Physiology and Genetics, SAV, Bratislava, Slovak Republic

Introduction: T-type calcium channels are distinguished by relatively low voltage threshold for an activation and steep voltage dependence of activation and inactivation kinetics just above the activation threshold. Further, while macroscopic current kinetics of $Ca_V3.1$ and $Ca_V3.2$ channels are virtually identical, kinetics of the $Ca_V3.3$ channel is almost one order more slow. Kinetics and voltage dependence of macroscopic inward calcium current through Ca_V3 channels was described in a detail. In contrast, very little information is available on gating current of these channels. Therefore we compared gating currents measured from all three $Ca_V3.1$, $Ca_V3.2$ and $Ca_V3.3$ channels.

Material and Methods: Gating current was measured by means of whole-cell patch clamp method. Bath solution contained (in mM): CsCl 105, HEPES 10, $CaCl_2$ 2, $MgCl_2$ 1, glucose 10, a TEA-Cl 40; pH 7.4 (CsOH). Pipette solution contained (in mM): CH_3SO_4Cs 130, Na-ATP 5, HEPES 10, TEA-Cl 10, EGTA 10, $MgCl_2$ 5; pH 7.4 (CsOH). Inward calcium current was blocked by 30 μM of $ErCl_3$. Charge-voltage (Q-V) relations were measured from a holding potential of -100 mV by series of 15 depolarizing pulses with amplitudes between -90 mV and +50 mV. Linear component of leak current and capacity transients at the beginning and the end of each depolarizing pulse were subtracted by P/8 method. Three consecutive runs were averaged for each pulse.

Results and Discussion: Voltage dependencies of macroscopic current activation are similar for all three Ca_V3 channels. However, while the gating kinetics of macroscopic calcium current is virtually identical for $Ca_V3.1$ and $Ca_V3.2$ channels, it is about one order slower for the $Ca_V3.3$ channel. Voltage dependencies of charge movement differ dramatically from those for macroscopic current. First, their slope factors are several-fold bigger that slope

factors of macroscopic current activation. Second, activation mid-point for $Ca_V3.3$ channels on-gating is shifted to more positive membrane potentials by about 20 mV compare to $Ca_V3.1$ and $Ca_V3.2$ channels, whose activation mid-points are similar. The same is truth for off-gating voltage dependences. Kinetics of both on- and off-gating is remarkably faster for $Ca_V3.1$ and $Ca_V3.2$ channels compare to $Ca_V3.3$ channels. Further, more charge is moved per unit of macroscopic current amplitude in $Ca_V3.3$ channels compare to $Ca_V3.1$ and $Ca_V3.2$ channels.

Conclusion: Significant differences in macroscopic inward current flowing through the Ca_V3 channels are reflected also in differences in charge movement reflecting voltage sensor movement in those channels. However, more differences are observable in charge movement than in macroscopic calcium current.

Acknowledgement
Supported by VVCE-0064-07 and VEGA 2/0195/10.

ULTRASTRUCTURAL CHANGES IN DYADS OF RAT MYOCYTES INDUCED BY A SINGLE DOSE OF ISOPROTERENOL

R. Kováč[2], I. Zahradník[1], M. Novotová[1]

[1]*Institute of Molecular Physiology and Genetics, Slovak Academy of Sciences, Bratislava, Slovak Republic,* [2]*Faculty of Pharmacy, Comenius University, Bratislava, Slovak Republic*

Introduction: Experimental myocardial injury and hypertrophy can be induced in rats by a single high dose of isoproterenol (ISO), and it is manifested in isolated ventricular myocytes by changes in calcium spikes activated by calcium current. Myocardial injury resulted in longer latencies of calcium spikes and induced a strong effect of the calcium current density on the latency and synchrony of calcium spikes (1). The aim of this study was to characterize ultrastructural changes of dyadic microdomains and relate them to the reduced E-C coupling efficiency.

Material and Methods: Male Wistar rats (200-250 g) were treated with a single s.c. dose of ISO (150 mg/kg b.w.) to evoke myocardial injury. On day 15 after ISO administration the hearts were excised, perfused retrogradely with calcium-free Tyrode solution to relax the heart, and fixed with 2% glutaraldehyde solution. The surviving tissue from the endocardial layer of the left ventricular free wall was dissected and processed for electron microscopy. The ultrastructure of myocytes was evaluated in ultrathin longitudinal sections at 15000× magnification using electron microscopy. The basic types of dyads were defined and changes in their occurrence were analyzed. The analyzed regions were located 5 μm below the sarcolemma to correspond to the location of calcium spikes in confocal microscopy measurements.

Results and Discussion: The myocardium of ISO-treated rats was slightly hypertrophic and showed clear signs of local injury near the apex, reminiscent of an infarcted region. Undamaged cardiomyocytes of ISO treated rats, localized in

the functional part of the left ventricles, displayed regions of developing hypertrophy but otherwise resembled myocytes of control rats.

Ultrastructural analysis revealed five types of dyadic complexes in control and in ISO-treated rats, differing in the appearance of their t-tubule and cisternal membranes and in their relative placement. Distortions in t-tubules involved the appearance of extrusions and caveolae. Distortions in cisterns involved fragmentation and detachment from the t-tubule. Interestingly, ISO treatment did not cause appearance of new, distorted types of dyads, neither their substantial dislocation from the position near the Z-lines of myofibrils, nor changes in their overall number. Instead, the effect of ISO was manifested in changes of the relative occurrence of individual types of dyads. While in control rats the optimal dyads dominated, contributing by about 75%, in ISO myocytes their occurrence was reduced to below 30%. Dyads with distorted t-tubules represented about 10% and 16% in control and ISO myocytes, respectively, while dyads with distorted cisternal membranes represented about 15% in control but up to 55% in ISO myocytes.

Conclusions: We conclude that the myocardial injury caused by ISO, manifested by impaired calcium signaling during excitation–contraction coupling, is accompanied by parallel changes in the morphological qualities of the dyadic complexes. It can be speculated that the quality of calcium signaling is closely related to the quality of its structural counterpart – the dyads.

Acknowledgement

This work was supported in part by grants VEGA 2/0174/09, VEGA 2/0102/08, APVV-0139-06 and by the European Union Contract No. LSHM-CT-2005-018833/EUGeneHeart.

References

[1] Zahradnikova A jr. et al., *J Physiol Sci* 59: Suppl. 1, p. 313 (2009).

ELECTRICAL PROPERTIES OF SINGLE MITOCHONDRIAL CHANNELS

K. Ondriaš, Z. Tomášková, V. Komínková, L. Máleková

Institute of Molecular Physiology and Genetics, SAV, Centre of Excellence for Cardiovascular Research, Bratislava, Slovak Republic

Introduction: Chloride channels regulate the movement of a major cellular anion, and thus regulate cellular and organellar membrane potential, transport, fusion, pH, cell cycle, cell volume, adhesion, and motility. This functional diversity leads to the involvement of chloride channels in the regulation of blood pressure, apoptosis, free radical release, reperfusion injury, and cardioprotection, in addition to roles in various cellular pathologies. Impaired chloride transport can cause a variety of diseases such as cystic fibrosis, myotonia, epilepsy, hyperekplexia, lysosomal storage disease, deafness, renal salt loss, kidney stones, and osteopetrosis. However, single channel properties of mitochondrial channels (mtCl) are mostly unknown. Therefore in the represent study we investigate their single channel properties and modulation by ATP and Mg^{2+}.

Material and Methods: The crude rat heart mitochondria and submitochondrial particles (innermembrane vesicles) from the crude mitochondria were isolated from the hearts of male Wistar rats. The vesicles containing chloride channels were fused into bilayer lipid membrane (BLM) and the single chloride channel currents were measured at 250/50 mmol/l cis/trans solutions.

Results and Discussion: We observed three different behaviors of the single channels. (1) Regular/classical mtCl channels, defined as channels having stable baseline, classical stable and constant opening and closing chloride current levels. (2) Ragged mtCl channels, defined as the highly fluctuating channels with a stable baseline, but lacking stable and constant opening and chloride current levels. (3) Promiscuous mtCl channels or channel complexes, defined as channels that suddenly switch between Cl^- and K^+ permeability with time or

under different physiological or pathological conditions (voltage, pH or oxidation status). The observed chloride channels (*n*=112) possessed wide variation of sensitivity to ATP. ATP (0.5-2 mmol/l) in a concentration dependent manner modulated and/or inhibited the chloride channel activities (*n*=38/112). ATP (0.5-2 mmol/l) without presence of Mg^{2+} decreased the chloride channel current amplitude (*n*=12/14), whereas Mg^{2+} significantly reversed the effect (*n*=4/4).

Conclusion: We suggest that the ATP-intracellular chloride channel interactions and Mg^{2+} modulation of the interactions may regulate different physiological and pathological processes.

Acknowledgement
Financial support by Slovak Science Grant Agency VEGA 2/0150/10 is gratefully acknowledged.

INFLUENCE OF IONIC LIQUIDS ON CONFORMATION TRANSITIONS OF CYTOCHROME C

J. Parnica[1], L. Kandráč[1], M. Antalík[1, 2]

[1]Department of Biochemistry, Faculty of Sciences, P.J. Safarik University, Kosice, Slovak Republic, [2]Institute of Experimental Physics, Slovak Academy of Sciences, Kosice, Slovak Republic

Introduction: Ionic liquids are materials with ionic character, yet are liquid at room temperature. Furthermore, depending on the cations and anions types in mixture, the hydrogen-bonding character and water miscibility can effectively be tuned to the application [1]. They have recently attracted much attention as "green" alternatives to conventional organic solvents in various fields including analytical chemistry and separation processes due to their unique properties such as high thermal stability, negligible vapor pressure and non-flammability [2-4]. Deep eutectic solvents (DES) are a new class of solvents typically formed by mixing choline chloride with hydrogen bond donors such as acids, amines and alcohols. Amino acids have both a carboxylic acid residue and an amino group in a single molecule, they can be used as either anions or cations in ionic liquids [5]. Most DES's are non-reactive with water, biodegradable, and have acceptable toxicity profiles [6].

We show that mixtures of substituted quaternary ammonium salts such as hydroxyethyltrimethylammonium (choline) chloride with urea, malonic acid and sorbitol in specific molar ratio produce eutectics that are liquid at ambient temperature and have unusual properties such as solvation of cellulosis.

Material and Methods: The original eutectic mixtures (DES) were formed by mixing the two components together in different molar ratios at 50-80°C until homogenous, colorless liquid formed.

Cyt-c (purity 95% based on H_2O content 2,8%) from horse heart was purchased from Sigma Co. and was used without further purification.

UV-vis absorption spectra (200-800 nm) of native cyt-c (1mM) in distilled water were measured at 25°C using a Jasco V-630 spectrophotometer. Circular dichroism (CD) and magnetic CD (MCD) spectra were monitored in Jasco J-815 spectropolarimeter.

Results and Discussion: We describe the stability and conformation transitions of a model protein, ferricytochrome c, in solution in choline chloride/urea, choline chloride/malonic acid and choline chloride/sorbitol.

Whereas pH conformation transition value of ferricytochrome c in H_2O with low salt concentration is 2.5, the value in ionic liquids shifts into the area of slightly acid pH.

This type of conformation transition is associated with the transition of low-spin state of Fe in ferricytochrome c into the mixture state (high- and low-spin state). The highly acid pH with the choline chloride present induces the origination of a unique spectrum of ferricytochrome c that is probably connected with the formation of a high-spin penta-coordinated Fe heme.

Conclusion: Ionic liquids have demonstrated to be interesting systems that enable to characterize new types of conformation states of ferricytochrome c.

Acknowledgement

This work was supported within the projects Nos., 26220120001, 26220220005, 2622022033 in frame of SF EU, Centre of Excellence of SAS Nanofluid and VEGA 0056, 0038 and 0079.

References

[1] Wasserscheid P., Welton T., Ionic liquids in synthesis. Weinheim: Wiley-VCH (2002).
[2] Shimojo K., Goto M., Anal. Chem., 76, 5039 (2004).
[3] Shimojo K., Nakashima K., Kamiya N., Goto M., Biomacromolecules, 7, 2 (2006)
[4] Kubota F., Goto M., Solv. Extr. Res. Dev. Jpn, 13, 23 (2006)
[5] Ohno H., Fukumoto K., Amino Acid Ionic Liquids, Accounts of Chemical Research 40 (11), 1122 (2007)
[6] Morrison H.G., Sun CH.C., Neervannan S., Characterization of thermal behavior of deep eutectic solvents and their potential as drug solubilization vehicles, International Journal of Pharmaceutics 378, 136 (2009).

LIPOPLEXES DNA – DOPC - GEMINI SURFACTANT: A SMALL ANGLE X-RAY DIFFRACTION AND FLUORESCENCE SPECTROSCOPY

L. Hubčík[1], P. Pullmannová[2], D. Uhríková[1], S. S. Funari[3], I. Lacko[1], F. Devínsky[1], P. Balgavý[1]

[1]Faculty of Pharmacy, Comenius University, Bratislava, [2]Faculty of Chemical and Food Technology, Slovak University of Technology, Bratislava, Slovak Republic, [3]Hasylab at DESY, Hamburg, Germany

Introduction: The DNA - cationic liposome aggregates (lipoplexes) are intensively investigated as potencial gene delivery vectors. The effective delivery vector should condense DNA rapidly, and to protect it against the degradation in plasma. The physico – chemical properties, and the microstructure of lipoplexes play a key role in trasfection efficiency. In present work we study DNA condensation as a function of the surface charge density of lipoplexes, and ionic strength of solution, using fluorescence spectroscopy. The structure of the lipoplexes was examinated using synchrotron small-angle X-ray diffraction. Cationic liposomes were prepared as a mixture of gemini surfactant (GS) ethane-α,ω-diyl-bis(dodecyl-dimethylammonium bromide) (C2GS12), amphiphilic molecule containing two head groups and two alkyl chains linked by a spacer. GS have shown good transfection activity *in vitro* and *in vivo* [1].

Material and Methods: The C2CS12, highly polymerized calf thymus DNA, and dioleylphosphatidylcholine (DOPC) were dissolved in 0.005 mol/l or 0.15 mol/l NaCl solution, respectively. DOPC unilamellar liposomes were prepared by extrusion of the lipid dispersion through a polycarbonate filters with pores of diameter 100 nm. The unilamellar liposomes were mixed with the solution of C2GS12 at various molar ratios and stored at 4 °C for 12 hours. DNA-DOPC-C2GS12 lipoplexes were prepared by mixing DNA solution with the C2GS12-DOPC liposomes. The fluorescence experiments were performed at the Fluoromax 4 spectrofluorometer (Jobin Yvon, France). DNA was labelled by

fluorescence probe ethidium bromide (EtBr). The emission fluorescence intensity was measured at λ_{em} = 596 nm, using exciting wavelength λ_{ex} = 520 nm. A small-angle (SAXD) synchrotron X-ray diffraction experiments were performed at the soft condensed matter beamline A2 at HASYLAB, DESY.

Results and Discussion: DNA polyanion interacts with cationic liposomes electrostatically. With increasing surface charge density of cationic liposomes, the fluorescence intensity of EtBr decreases. The binding sites of DNA become unaccessible to the EtBr probe due to DNA condensation by DOPC-C12GS liposomes. The effect depends on the ionic strength of the solution. The SAXD experiments revealed a condensed lamellar phase in DNA-DOPC-C2GS12 lipoplexes. The DNA strands are packed regularly (d_{DNA} spacing) in water phase between the lipid bilayers characterized by the periodicity d. The repeat distance d varied in the range 6.7 – 6.1 nm with the increasing C2GS12 : DOPC molar ratio. The distance between DNA strands d_{DNA} varied in the range 4.9 – 3.1 nm and depends on the C2GS12 : DOPC molar ratio too. Both paramaters, d and d_{DNA} show dependence on used ionic strength of solution, however the effect is not significant.

Conclusion: Both, structural parameters of lipoplexes as well as the DNA condensation depends on surface charge density of cationic liposomes. The structural parameters of the lipoplexes has shown only minor dependence on used ionic strength of solution. This stability can be responsible for their good transfection effectivity documented in [1].

Acknowledgement

The research leading to these results has received funding from the European Community's Seventh Framework Programme (FP7/2007-2013) under grant agreement n° 226716 (HASYLAB project I-20080187 EC), by the JINR project 07-4-1069-09/2011, and by the VEGA grant 1/0292/09 to DU.

References

[1] S. D. Wettig, R. E. Verrall, and M. Foldvari, Current Gene Therapy **8**, 9 (2008).

LOCALIZATION OF CIS-PLATINUM IN MOUSE NEOPLASTIC CELLS L1210

A. Rusnák, L. Gibalová, Z. Sulová, A. Breier, B. Uhrík

Institute of Molecular Physiology and Genetics, SAV, Bratislava, Slovak Republic

Introduction: Multidrug resistance (MDR) is a phenomenon, which emerges following exposure of a cancer cell to a certain kind of cytostatic agent. Subsequently, the cell becomes cross-resistant to other cytostatics, which are structurally as well as functionally different from the original cytostatic agent. One of the most common causes of this phenomenon is the expression of P-glycoprotein (P-gp). Many MDR cells exhibit a resistance to apoptotic processes (programmed cell death). With transmission electron microscopy (TEM) the changes in ultrastructure of the cell exposed to cytostatic agents may be observed and the early stages of the mechanisms of cell death (apoptosis, necrosis, autophagy) may be differentiated. Other cytochemical methods are more suitable to quantify the number of apoptotic and necrotic cells.

Material and Methods: In this study, three lines of mouse leukemic cells L1210 were examined: parental sensitive line (S); a sub-line derived from S, cultivated in absence of cytostatic agent vincristine (R); the same cell line cultivated in presence of vincristine (V) and the cells transfected by a gene for human P-glycoprotein (T). During the experiment, the cells were exposed for 24 hours to cytostatic agent cis-Platinum (cis-Pt), cis–$[Pt(NH_3)_2Cl_2]$, which is not a substrate to P-gp. TEM samples were prepared by standard methods. The samples designated for localization of cis-Pt were not contrasted, since it was assumed that heavy metals used for contrasting might overlay the contrast of cis-Pt. This assumption was experimentally confirmed.

The ultrathin sections were examined under an electron microscope JEOL JEM 1200 EX at 80 kV. The study of overall morphological changes and the

count of cellular organelles was done at the magnification of 7500×; for the localization of cis-Pt the magnification of 60,000× was used.

Results and Discussion: Exposure to cis-Pt increased the mitochondria count in surviving cells of all cell types (S, R, V, and T). It was possible to observe early as well as late apoptosis stages, which were almost absent in the control cell group. In dead cells, it was not always possible to determine unequivocally the mechanism of the cell death (apoptosis or necrosis). Cis-Pt in all types of cells (S, R, V, and T) was located in cytoplasm as well as in the nucleus. According to evaluated images, the cis-Pt was not freely suspended in cytoplasm, but it was bound to rough endoplasmic reticulum and mitochondrial cristae. The occurrence in Golgi complex could not be confirmed due to lower level of contrast. The occurrence of cis-Pt in autophagic vesicles was evident. In the nucleus, the cis-Pt was markedly bound to heterochromatin; it was less abundant in euchromatin. In the nucleus, it was possible to observe spatially larger cis-Pt agglomerates, around which the count of cis-Pt particles was lower. The localization of cis-Pt in cell membranes was not confirmed. It may be assumed that the diffusional transport of cis-Pt across the cell membrane enables its free penetration into the cytoplasm.

Conclusion: Cis-Pt evidently causes an onset of the apoptosis in parental cells as well as in cell lines with the MDR phenotype; it was confirmed also by other cytochemical methods. The differences in the apoptosis onset, which were determined by Annexin V and propidium iodide binding to cells, were not observable by electron microscopy.

Acknowledgement
This work was supported by grants: APVV-0084-07, VEGA 2/7122, 2/6080 a VVCE 0064-07.

THE STUDY OF OPTICAL PROPERTIES OF Mn-DOPED ZINC OXIDE NANOPARTICLES

M. Šimšíková[1], M. Antalík[1,2]

[1]Department of Biochemistry, Faculty of Science, P. J. Safarik University, Kosice, Slovak Republic, [2]Institute of Experimental Physics, SAV, Kosice, Slovak Republic

Introduction: Biosensoring is very attracted for applications in genetic, pathology, criminology, safety of food and many other industries. Zinc oxide represent a new class of materials with high potential for biosensoring due to its unique properties and biocompatibility (zinc is a very important trace element in humans and plays an important part in many biological systems).

Very widely used method to improve the electrical, optical and magnetic properties of semiconductors, which is crucial for its practical applications, is doping - the intentional introduction of impurities into a material.

However, research on ZnO for bio-applications considerably lags behind the other candidates because the synthesis is not as well developed, and the doping and surface modification of ZnO are less well understood. In this paper, we studied the photoluminescent properties of ZnO nanoparticles doped by Mn.

Material and Methods: The Mn-doped nanoparticles of ZnO were prepared by dissolving of NaOH in ditlilled water (0,13 M, 75 ml) and after one hour of continuously stirring $ZnCl_2$ was added to the solution (0,4 M, 5 ml). To dope ZnO nanoparticles with potassium permanganate $KMnO_4$ was dissolved in distilled water (6 mM, 30 mM, 60 mM; 15 ml) and was added to the stirring solution of zinc chloride. After three hours of constant stirring a ligh pink / pink / purple solution was obtained. The precipitate was washed in distilled water and then the water was allowed to evaporate at room temperature to obtain doped Mn-ZnO nanoparticles.

Results and Discussion: The optical properties of prepared nanoparticles were characterized by methods of UV-VIS spectroscopy and photoluminiscence.

Photoluminescence spectra of the undoped and capped ZnO nanoparticles were measured under UV (350 nm) excitation and compared in figures 1(a)–(d). As seen in figure 1(a), pure ZnO emits at 580 nm which corresponds to the the green emission. The PL spectra of nanoparticles doped by Mn were changed. The most interesting was PL spectrum of Mn-doped nanoparticles, where we used 6 mM solution of $KMnO_4$ (1(b)). A major benefit of doping was new red emission peak at 770nm.

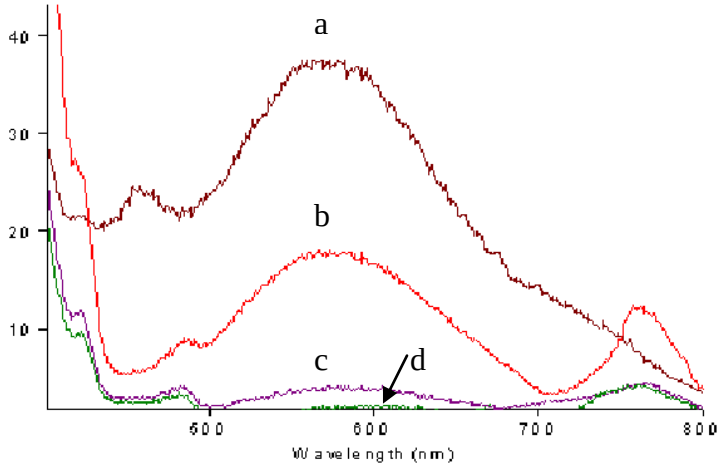

Figure 1. Emission spectrum undoped and doped ZnO nanoparticles a) undoped ZnO, b) ZnO with 6 mM KMnO4, c) 30 mM KMnO4, d) 60 mM KMnO4.

Figure 2. Undoped and Mn-doped ZnO samples

Conclusion: We prepared ZnO nanoparticles doped with Mn in the presence of potassium permanganate. The results presented above show that the assistance of $KMnO_4$ induced the bandgap modification and PL emission has been redshifted.

Acknowledgement
This work was supported by the research grants from the Slovak Grant Agency VEGA No. 0038, 7055, 0056 and by Slovak Academy of Science in frame of CEX NANOFLUID, projects ESF 26220120021 and NFP 26220220005.

EFFECT OF PHYTOALEXINS ON INSULIN AMYLOID AGGREGATION

K. Šipošová[1], A. Antošová[2], P. Kutschy[1], Z. Daxnerová[3], Z. Gažová[2]

[1]Institute of Chemical Sciences, [3]Institute of Biology and Ecology, Faculty of Science, P. J. Safarik University, Kosice, Slovakia, [2]Department of Biophysics, Institute of Experimental Physics SAS, Kosice, Slovakia

Introduction: Protein misfolding and formation of linear β-sheet-rich structures, the so-called amyloid aggregates, are closely associated with more than 20 human disorders, such as Alzheimer′s and Parkinson′s diseases, "prion"-associated Creutzfeldt–Jakob disease and diabetes type II. A number of structurally different proteins are known to form amyloid aggregates including insulin. Amyloid deposits of insulin have been observed in patients with diabetes after subcutaneous insulin infusion and after repeated injection [1]. Presence of insulin aggregates has toxic consequence to cells and can act as nucleus promoting formation of amyloids from other proteins. Thus, prevention of insulin amyloid fibrillation can play important role in the treatment of diabetes mellitus. Phytoalexins are antimicrobial low molecular weight secondary metabolites, produced by plants after their exposure to biological or physical stress [2]. We have decided to investigate effect of these compounds on amyloid aggregation of human insulin.

Material and Methods: Insulin was dissolved to final concentration of 10 μM in 100 mM NaCl, pH 1.6. To form amyloid aggregates the protein solution was incubated in the absence or in the presence of 200 μM phytoalexins at 65°C and stirred constantly (1200 rpm) for 120 min. ThT assay was used for investigation of the compound ability to inhibit formation of amyloid aggregates as the ThT fluorescence is proportional to amount of amyloid aggregates. ThT was added to protein solution in a final concentration of 20 μM. Fluorescence intensity was measured at excitation of 440 nm and emission of 485 nm. The ability of the

most effective phytoalexin derivatives to inhibit formation of insulin fibrils was confirmed by transmission electron microscopy.

Result and Discussion: To make primary screening we tested the ability of phytoalexin derivatives to inhibit formation of insulin amyloid aggregates (Iagg) in presence of 200 μM phytoalexin compounds by ThT fluorescence assay. The inhibiting activity was quantified as percentage of maximal ThT fluorescence observed for insulin amyloid aggregates alone. We have found that benzocamalexin and cyclobrassinin inhibit insulin aggregation very effectively (~ 80 % and 75% inhibiting activity).

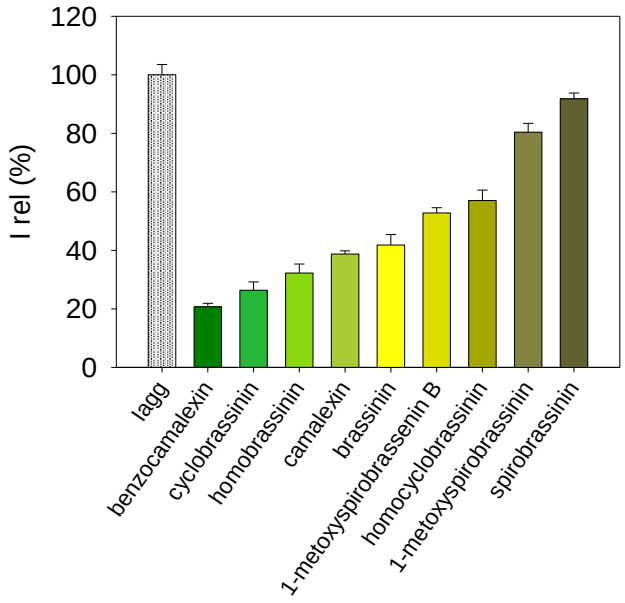

Figure: Inhibition of insulin amyloid aggregation by phytoalexins observed by ThT assay. The fluorescence was normalized to the signal detected for insulin amyloid aggregates (Iagg).

Conclusion: We identified very effective inhibitors of insulin fibrillization characterized by inhibiting activity at low micromolar concentration. Our data suggest potential therapeutic use of benzocamalexin and cyclobrassinin in prevention of insulin amyloid aggregation.

Acknowledgement

This work was supported within the projects Nos. 26220220005, 26220120033 in frame of SF EU, Centre of Excellence of SAS Nanofluid and VEGA 0079, 0056 and 0038.

References

[1] Dische, F. E. et al. Diabetologia, 1988, 31, 158–161

[2] Daniel, M., Purkayastha, R. P., Progress in Phytoalexin Research during the Past 50 Years In Handbook of Phytoalexin Metabolism and Action; Eds.; Marcel Dekker: New York, 1995; p. 1

THE EFFECT OF LUMINAL Ca^{2+} ON THE CARDIAC RYANODINE RECEPTOR IN THE PRESENCE OF 2.5 mM ATP

B. Tencerová, M. Gaburjaková, A. Zahradníková

Institute of Molecular Physiology and Genetics, SAV, Bratislava, Slovak Republic

Introduction: The ryanodine receptor (RyR2) is a Ca^{2+} activated, Ca^{2+} permeable channel of the sarcoplasmic reticulum (SR) that mediates calcium induced calcium release (CICR) in the cardiac muscle cells. Although activity of RyR2 channels is primarily controlled by cytosolic Ca^{2+}, it was found that Ca^{2+} in the lumen of the SR serves not only as storage of Ca^{2+} for subsequent release but also participates in regulation of the RyR2 channel activity [1-3] as a strong stimulator of CICR and one of the determinants of excitation-contraction coupling gain. Therefore we tested the effect of luminal Ca^{2+} on activity and sensitivity of the RyR2 channel to adenosine triphosphate (ATP), which in millimolar quantities seems to be a very effective coactivator of RyR2 [4, 5].

Material and Methods: RyR2 channels from rat cardiac microsomes were reconstituted into bilayer lipid membranes (BLM). Single-channel currents were recorded under voltage-clamp conditions at a membrane potential of 0 mV in asymmetric *trans*/*cis* environment. The *trans* chamber, corresponding to the SR lumen, contained 50 mM KCl, 250 mM HEPES, and different concentrations of $Ba(OH)_2$ and/or $Ca(OH)_2$ (pH 7.35). The *cis* chamber, corresponding to the cytosolic side, contained 1 mM EGTA, 125 mM Tris, 50 mM KCl, 250 HEPES and either 0.5 or 0.629 mM $CaCl_2$, corresponding to 90 and 200 nM free Ca^{2+}, respectively. As soon as a RyR2 channel was incorporated into the BLM, recording of channel current was started. At first, RyR2 channel activity was recorded in the absence of Na_2ATP, and then increasing concentrations of Na_2ATP were successively applied to the cytosolic side.

Results and Discussion: We investigated the effect of luminal Ca^{2+} on the open probability (P_O) of the RyR2 in the presence of physiological concentration of ATP (2.5 mM) and diastolic cytosolic Ca^{2+} (90 nM free). We found that P_O was gradually enhanced with increasing luminal Ca^{2+} from 0 mM to 53 mM. The presence of 1 mM luminal Ca^{2+} (estimated physiological concentration) had only a slight but significant effect on P_O, while 53 mM luminal Ca^{2+} increased P_O markedly. Therefore we were interested whether 1 mM luminal Ca^{2+} is able to increase the open probability of RyR2 to a higher extent at elevated, but subactivating, cytosolic Ca^{2+}. In the presence of 2.5 mM ATP, the increase of luminal Ca^{2+} from 0 mM to 1 mM or the increase of cytosolic Ca^{2+} from 90 nM to 200 nM significantly elevated P_O. When both luminal Ca^{2+} (1 mM) and cytosolic Ca^{2+} (200 nM) were present, P_O of RyR2 was significantly enhanced. However, the effects of luminal and cytosolic Ca^{2+} were not additive; rather, luminal and cytosolic Ca^{2+} interacted in ways that amplified their individual effects.

Conclusion: The changes of P_O of RyR2 induced by luminal as well as by cytosolic Ca^{2+} in the presence of 2.5 mM ATP were significant and may contribute to regulation of diastolic Ca^{2+} spark frequency under normal as well as pathological conditions.

Acknowledgement
This work was supported in part by the EU Contracts No. LSHM-CT-2005–018802/CONTICA and LSHM-CT-2005–018833/EUGeneHeart and by the grants APVV-0139-06 and VEGA 2/0190/10.

References
[1] Sitsapesan R,. Williams AJ: *J Membr Biol* 137: 215-26, 1994.
[2] Tripathy A, Meissner G: *Biophys J 70*: 2600-15, 1996.
[3] Laver DR: *Biophys J* 92: 3541-55, 2007.
[4] Copello JA et al.: *J Membr Biol* 187: 51-64, 2002
[5] Kermode H, Williams AJ, Sitsapesan R: *Biophys J* 74: 1296-304, 1998.

STUDY OF THE ULTRASENSITIVITY OF THE BCL-2 APOPTOTIC SWITCH

T. Tokár, J. Uličný

Department of Biophysics, Faculty of Science, University of P. J. Safarik, Kosice, Slovakia

Introduction: Bcl-2 apoptotic switch is important control mechanism regulating crucial event of apoptosis - permeabilization of outer mitochondrial membrane. Biological switches such as Bcl-2 apoptotic switch are molecular mechanisms converting continuous incoming signals to two mutually distinct outputs, ensuring unambiguous transitions between two different cellular states. One of the necessary requirements to generate this behavior is ultrasensitive reaction mechanism. There are two competing hypotheses regarding its internal working - the indirect and direct activation.

Material and Methods: Based on hypotheses of direct and indirect activation, we constructed corresponding mathematical models of Bcl-2 apoptotic switch. Moreover, we introduced third, hybrid model involving controversial interactions from both, indirect and direct model. In this work we utilized ultrasensitivity of the Bcl-2 apoptotic switch models as a criterion, against which we judge plausibility of its models. For each model we analyzed its robustness with respect to its ability to preserve ultrasensitivity against variations of its reaction parameters and initial conditions around estimated reference values. We have analyzed influence of the most debatable reactions on the behavior of our models.

Results and Discussion: As the results of robustness analysis show, it is very improbable that the indirect model, as examined in our work, could act as biological switch mechanism. Moreover, we have found that, while reaction specific for the direct model has particularly beneficial effect on ultrasensitivity of the Bcl-2 apoptotic switch, reactions proposed by the indirect model seems to

reduce sensitivity in very strong manner.

Conclusion: The direct model as we proposed in this work, can act as biological switch, under sufficiently wide range of parameter settings. We found other, alternative variants as inappropriate, since unable to resemble requested behavior.

Acknowledegments
This work was financially supported by grants VEGA-1/4019/07; APVV-0449-07 and VVGS PF 12/2009/F. This work could not be done without scholarships granted to Tomas Tokar from National Scholarship Programme of the Slovak Republic and "Hlavicka" scholarship from Slovensky plynarensky priemysel a.s., we wish to thank for this support. Tomas Tokar appreciate many valuable discussions with colleagues from Institute for Systems Theory and Automatic Control, University of Stuttgart, Germany.

N-ACETYL-L-CYSTEINE INTERACTS WITH NaHS INDUCED RELEASE OF NO

Z. Tomášková[1], A. Špániková[1,2], S. Cacanyiova[3], P. Dočolomanský[1], K. Ondriaš[1]

[1]Institute of Molecular Physiology and Genetics, SAV, Centre of Excellence for Cardiovascular Research, Bratislava, Slovak Republic, [2]Institute for Heart Research, SAS, Bratislava, Slovak Republic; [3]Institute of Normal and Pathological Physiology, SAV, Bratislava, Slovak Republic

Introduction: N-acetyl-L-cysteine is an endogenous compound, but it is also used for treatment of paracetamol poisoning. Except of beneficial effects, many adverse reactions are related to this treatment. Intravenous administration of NAC was reported to decrease systemic vascular resistance during brief hyperoxia in cardiac risk patients. In experimental models of hypertension (rats), NAC had hypotensive effect, probably by affecting nitric oxide and adrenergic pathways. NAC caused a relaxation of aorta, also after endothelium removal. All these findings indicate a possible role of NAC as a vasoactive agent or as a molecule interfering with different pathways of vascular tone regulation. Since we have previously found that sodium hydrogensulphide (NaHS) released NO from S-nitrosoglutathione (GSNO), it was of our interest to study whether NAC can interfere with the NaHS caused NO release.

Material and Methods: UV-vis spectroscopy was used in order to investigate the evolution of the chemical reaction and its kinetics. We monitored the interaction of NaHS with GSNO and the effect of NAC on this interaction. The reaction was studied in solutions with different pH: 6.0, 7.4 and 8.0. All three solutions contained (in $mmol.l^{-1}$): 160 KCl, 1 $MgCl_2$, 0.1 DTPA. The pH was adjusted by HEPES and Tris or PIPES and Tris to the chosen value. The concentrations of NaHS and GSNO were 200 $\mu mol.l^{-1}$ and NAC concentrations were 200 and 400 $\mu mol.l^{-1}$. We focused on the absorbance at 334 nm, which

reflects the amount of S-NO bond. Using Griess reagent, we monitored the amount of released NO. In these experiments, the concentration of NaHS and GSNO were 100 μmol.l^{-1} and NAC was added in concentration range from 40 to 3200 μmol.l^{-1}.

Results and Discussion: Using UV-vis spectroscopy, we found that NaHS effectively induced NO release from GSNO at 7.4 pH and it had negligible effects at 6.0 pH. Thus we confirm that the active form that causes the release of NO from GSNO is HS^- and not H_2S. We found that NAC slowed or inhibited NaHS induced NO release from GSNO at 7.4 and 8.0 pH, but increased NO release at 6.0 pH. These results indicate that NAC is involved in NO production induced by NaHS and that its effect is pH dependent. The experiments with Griess reagent indicated that NAC might be interacting with NaHS in a way that it allows only a small amount of HS^- left to interact with GSNO.

Conclusion: We have shown that the endogenous and commonly used antioxidant, NAC, by affecting the NaHS/GSNO interaction, interfered with the NO production from GSNO. We assume that these effects of NAC may explain in part its biological vasoactive effects. However, details and significances of the NAC-NO-NaHS reactions and a role of NAC as a modulator of the two vasorelaxing gasotransmitters – NO and H_2S/HS^- are still unknown.

Acknowledgement
Supported by VEGA No. 2/0150/10.

VISUALIZATION OF MITOCHONDRIA SPATIAL DISTRIBUTION IN LIVING CELLS

P. Topor[1], A. Mateašík[2], L. Bacharová[2]

[1]*Faculty of mathematics, physics and informatics, Comenius University, Bratislava, Slovak Republic,*

[2]*International Laser Centre, Bratislava, Slovak Republic*

Introduction: Mitochondria play a crucial role in cell energy metabolism. Mitochondrial disorders encompass diseases with common clinical manifestations [1] - neurological or heart related diseases. Functional state of mitochondria is supposed to be closely related to morphology and spatial organization of mitochondria networks [2]. Investigation of stained mitochondria using histological dyes based on Rhodamine showed to be toxic for the cell [3], so nowadays fluorescence protocols are being used. Mitochondria dimensions are in scale around 1 μm, what is beyond resolution of conventional fluorescence microscopes and very close to the resolution of confocal microscope. Therefore, the focus is on the improvement in resolution to provide valuable details for mitochondria network visualizations. Deconvolution algorithms are capable of removing noise, blur and out-of-focus light from measured data and thus effectively improve overall resolution of data.

Material and Methods: Cells of U-87-MG line stained with JC-1 marker were scanned using Zeiss LSM510 Meta confocal microscope into 3D stacks and consecutively processed using in-house developed software tool. Our tool implements: Total Variation -, Tikhonov-Miller- and custom-regularized versions of Richardson-Lucy (RL) deconvolution algorithm in order to reduce the artifacts triggered off by unregularized RL algorithm. Extended feature of our tool is the capability of streamed processing of large data sets. Mathematically estimated point spread function and experimentally measured

one was used in computations. The effect of restoration algorithms on visualization of mitochondria networks was evaluated.

Results and Discussion: Visualized mitochondria networks resembled the published spatial organization. The achieved improvement in data resolution revealed greater details in network organization, but on the other hand, artifacts creation should be carefully treated as it produces new type of problems to deal with. Further improvement of processing is discussed in detail and proposed for suggested areas (e.g. various scanning parameters) for future work.

Conclusion: The presented method of processing and visualization of mitochondrial data is suitable for examining response of mitochondria network organization in various conditions and its further improvement is a solid basis for artificial model creation.

Acknowledgement
We gratefully appreciate Dr. Slavka Kascakova for sample preparation. This work was supported by grant VEGA 1/0530/09.

References

[1] Tanji K., et al., Methods 46: 274-280, 2008.
[2] Benard G., et al., J. Cell Sci. 120: 838-848, 2007.
[3] Johnson L. V., et al., Proc. Natl. Acad. Sci. USA 77 (2): 990-994, 1980.

QUANTITATIVE MODELING OF APOPTOSIS – TNFR1 PATHWAY

C. Uličná[1], J. Uličný[1]

[1]*Department of Biophysics, Institute of Physics, University of P.J.Šafárik, Košice, Slovak Republic*

Introduction: Quantitative modeling of reaction kinetics is powerful tool for understanding of molecular interaction networks (Palsson). Carefully constructed and iteratively refined models reflect most important properties and dynamics of such networks in very compact unambiguous form and allow for prediction of experimental outcomes. In our contribution, we will present such model for particular problem of practical importance – the molecular interaction network processing TNFα signal through TNFR1 pathway. TNFR1 is one of the TNFR family of receptors, possessing death domain. Interaction between the cytokine ligand TNFα with TNFR1 triggers series of events associated with cell proliferation and apoptosis.

Material and Methods: We have created unified interaction network starting from known partial models, dealing with particular aspects of the TNFR1 pathway (Rangamani, Albeck). Existing models were rewritten using SBML formalism and simulated numerically using Copasi simulation framework and deterministic LSOD propagator. The results of simulations for known scenarios were compared to published results. This proved to be very useful in order to resolve ambiguities, spot typographic errors and to assure the equivalence of the model in new formalism. The part of molecular reactions treating endocytosis, as well as missing interaction parts, were written from scratch, using qualitative reaction data and extensive literature search. Missing concentrations and reaction rates were estimated using known physiological ranges for similar reactions (Aldridge), complemented by numerical simulations of common experimental scenarios.

Results and Discussion: The resulting model is fairly large – it comprises more than 90 molecular species (and their temporary complexes) involved in more than 60 reactions. The model explicitly accounts for and correctly predicts the following processes: TNFα binding to TNFR1 receptor triggers the sequence of signaling events associated with both cell proliferation and apoptosis. While the first event, activation of the transcription factor NFκB causing the activation of anti-apoptotic genes starts immediately upon receptor activation, the second event requires internalization of the receptor-ligand complex through clathrin-coated pits. Endocytosis, accompanied by ubiquitination and subsequent degradation of RIP1 protein – which forms part of the receptor-ligand complex – counteracts proliferation signaling and allows for activation of initiation caspase 8. Caspase 8, in turn, activates the effector caspase 3 (extrinsic apoptotic pathway) and/or cathepsin-ceramid cascade, which is mediating the Bid truncation to tBid (intrinsic apoptotic pathway).

Conclusion: We have constructed comprehensive model of the molecular reaction network, accounting for three known outcomes of events following the TNFα binding by TNFR1 receptor. While sufficiently generic, the model allows – provided sufficient cell-line characteristic experimental inputs – to make specific experimental predictions.

Acknowledgement
This work was financially supported by grants VEGA-1/4019/07 and APVV-0449-07.

References

[1] Palsson, B.O. *Systems Biology: Properties of Reconstructed Networks*. (Cambridge University Press: 2006).
[2] Physicochemical modeling of cell signaling pathways, Bree B. Aldridge, John M. Burke, Douglas A. Lauffenburger & Peter K. Sorge, Nature Cell Biology 8, 1195 - 1203 (2006)
[3] Survival and apoptotic pathways initiated by TNF-alpha: Modeling and predictions,Bree B. Aldridge, John M. Burke, Douglas A. Lauffenburger & Peter K. Sorge, Biotechnology and Bioengineering,vl 97, no 5, 1216-1229(2006)
[4] Modeling a snap-action, variable-delay switch controlling extrinsic cell death, Albeck JG, Burke JM, Spencer SL, Lauffenburger DA, Sorger PK., PLoS Biol. 2008 Dec 2;6(12):2831-52
[5] Impact of TNF-R1 and CD95 internalization on apoptotic and antiapoptotic signaling, Schütze S, Schneider-Brachert W., Results Probl Cell Differ. 2009;49:63-85.

RECRUITMENT OF RYANODINE RECEPTOR CHANNELS DURING CALCIUM SPARKS

I. Zahradník[1], I. Valent[1,2], A. Zahradníková[1]

[1]*Institute of Molecular Physiology and Genetics, Slovak Academy of Sciences, Bratislava, Slovak Republic,* [2]*Department of Physical and Theoretical Chemistry, Faculty of Natural Sciences, Comenius University, Bratislava, Slovak Republic*

Introduction: Elementary calcium release events, observed as calcium sparks, arise by activation of RyR channels in the calcium release unit (CRU). CRUs contain 50 – 200 RyRs [1]; however, according to recent studies [2], only a small fraction of them activates during the spark. These data are incompatible with calcium induced calcium release mechanism of CRU activation [3] due to the strong positive feedback given by very fast calcium activation of RyRs that should cause activation of all RyRs after opening of the first RyR in the CRU. In this work we provide theoretical analysis of CRU activation during calcium sparks based on a ryanodine receptor (RyR) gating model.

Material and Methods: The allosteric gating model of the ryanodine receptor calcium release channel [4] incorporating interaction of the RyR with Mg^{2+} [5] was used for description of CRU activation. The system of model equations was solved in Mathematica (Ver. 6.0.1, Wolfram Research, Champaign, IL) as previously described [4], thus giving formulae for the steady-state probabilities of RyR occurring in the states of interest. Fitting and analyses were carried out using the program Origin (Ver. 7.5, OriginLab, Northampton, MA).

Results and Discussion: The observed calcium release fluxes of repeatedly triggered calcium sparks [2] had a quantal character with a binomic distribution that corresponded to a very small number of open RyRs in the CRU. The distribution could be quantitatively reproduced using the RyR gating model if limited unbinding of Mg^{2+} during the spark was allowed. We found that

spontaneous sparks are most frequently evoked by random openings of the highly populated but very rarely opening Mg_4RyR and $CaMg_3$RyR forms, while triggered sparks by random openings of the very poorly populated but much more readily opening Ca_2Mg_2RyR and Ca_3MgRyR forms that form in response to the triggering Ca^{2+} influx. Only ~25% of RyR activation sites occupied by Mg^{2+} ions will liberate Mg^{2+} in response to the increase of dyadic Ca^{2+} evoked by the opening of the first RyR in the CRU. As a result, sparks triggered by calcium influx through voltage-dependent calcium channels are initiated by openings of the scarce but readily opening RyRs that have managed to liberate 1 – 2 Mg ions and bind 2 – 3 Ca ions. Furthermore, only 0.5 – 4% of RyRs in the calcium release unit manages to open during either a spontaneous or a triggered spark. On the basis of kinetic considerations, analysis of RyR gating during sparks enabled estimation of the rate of Mg^{2+} unbinding from the RyR activation sites, ${}^{Mg}k_{off} \approx 50\ s^{-1}$.

Conclusions: The unexpectedly low calcium release flux during calcium sparks can be explained by a RyR gating model involving allosteric interaction of Ca^{2+} and Mg^{2+} ions at RyR activation site. The resulting model of the calcium release unit unifies the theory of calcium signaling in resting and contracting cardiac myocytes.

Acknowledgement
This work was supported in part by the EU Contracts No. LSHM-CT-2005–018802/CONTICA and LSHM-CT-2005–018833/EUGeneHeart and by the grants APVV-0139-06, VEGA 2/0102/08 and VEGA 2/0190/10.

References

[1] Franzini-Armstrong C, Protasi F, Ramesh V. *Biophys J* 77: 1528-1539, 1999
[2] Wang SQ, Stern MD, Rios E, Cheng H. *Proc Natl Acad Sci USA.* 101: 3979-3984, 2004.
[3] Fabiato A. *J Gen Physiol* 85:247-289, 1985.
[4] Zahradník I, Györke S, Zahradníková A: *J Gen Physiol* 126: 515–527, 2005
[5] Zahradnikova A et al: *Am J Physiol* 285: C1059-1070, 2003.

RYANODINE RECEPTOR GATING AND ACTIVATON OF SPONTANEOUS CALCIUM SPARKS

A. Zahradníková[1], I. Valent[1,2], I. Zahradník[1]

[1]*Institute of Molecular Physiology and Genetics, Slovak Academy of Sciences, Bratislava, Slovak Republic,* [2]*Department of Physical and Theoretical Chemistry, Faculty of Natural Sciences, Comenius University, Bratislava, Slovak Republic*

Introduction: In cardiac muscle, the spontaneous calcium release events, observed as calcium sparks, are a key regulator of sarcoplasmic reticulum calcium content and represent the basic mechanism of priming calcium reserves for stimulated contraction. It was shown that calcium sparks appear due to opening of ryanodine receptors (RyRs) without the need of a external trigger. It is not clear, whether this spontaneous activity of RyRs is compatible with recent understanding of RyR gating. In this work we provide theoretical description of calcium sparks activation based on ryanodine receptor (RyR) gating model.

Material and Methods: A mathematical model of cardiac couplon was developed to compare the gating properties of ryanodine receptor calcium release channel and the measured frequency of spontaneous calcium sparks. It was assumed that (a) opening of a single RyR is sufficient to activate the calcium spark [1]; (b) at diastolic calcium levels, individual calcium sparks are independent [2]; and (c) the whole couplon becomes refractory for a certain time interval after the spark [3]. RyR models, in which channel opening was coupled either to calcium binding [4], or could occur only after occupation of all activation sites by Ca^{2+} [5], as well as the inhibitory effect of Mg^{2+} [6] were explored. The system of equations of individual RyR gating schemes was solved in Mathematica (Ver. 6.0.1, Wolfram Research, Champaign, IL) as previously described [1], thus giving formulae for the steady-state probabilities of RyR

occurring in the states of interest. Fitting and analyses were carried out using the program Origin (Ver. 7.5, OriginLab, Northampton, MA).

Results and Discussion: The calcium dependence of the frequency of spontaneous sparks observed in experiments [7] could be described only by models that included allosteric interaction between binding of Ca^{2+} to the activation sites and channel opening. Models that did not account for Mg^{2+} inhibition could describe this dependence if the fraction of functional RyR channels at the release sites was decreased to < 10%. Inclusion of both, the allosteric interaction and the binding of Mg^{2+} to activation and inhibition sites [6], led to quantitative correspondence between the data and model predictions. Analysis of the distribution of RyR states revealed that at rest, RyRs are almost fully occupied by Mg^{2+}. Therefore, spontaneous sparks are most frequently evoked by random openings of the RyRs occupied by 3 – 4 Mg ions.

Conclusions: Our results revealed two new determinants of RyR gating important for proper spontaneous calcium spark generation. The allosteric interaction between Ca^{2+} binding and RyR channel opening is responsible for the observed quasilinear calcium dependence of calcium spark frequency, allowing regulation of calcium leak throughout the diastolic range of cytosolic Ca^{2+} concentration. Steady-state inhibition by Mg^{2+} ions under diastolic conditions keeps the diastolic calcium leak at low level and thus prevents inadvertent activation of calcium release.

Acknowledgement
This work was supported in part by the EU Contracts No. LSHM-CT-2005–018802/CONTICA and LSHM-CT-2005–018833/EUGeneHeart and by the grants APVV-0139-06, VEGA 2/0102/08 and VEGA 2/0190/10.

References

[1] Stern MD et al.: *J Gen Physiol.* 113: 469-489, 1999
[2] Cannell MB, Cheng H, Lederer WJ: *Science*. 268: 1045-1049, 1995.
[3] Sobie EA, Song LS, Lederer WJ: *J Physiol*. 565:441-447, 2005.
[4] Zahradník I, Györke S, Zahradníková A: *J Gen Physiol.* 126: 515–527, 2005
[5] Zahradnikova, A et al.: *J. Gen. Physiol.* 114: 787-798, 1999.
[6] Zahradnikova A et al: *Am. J. Physiol.* 285: C1059-1070, 2003.
[7] Lukyanenko VI, Gyorke S: *J. Physiol.* 521: 575-585, 1999

EVIDENCE FOR IMPAIRED LOCAL EXCITATION-CONTRACTION COUPLING IN ISOPROTERENOL-INDUCED MYOCARDIAL INJURY

A. Zahradníková jr., E. Poláková, I. Zahradník, A. Zahradníková

Institute of Molecular Physiology and Genetics, SAV, Bratislava, Slovak Republic

Introduction: In different models of left ventricular hypertrophy and heart failure, impairment of excitation-contraction coupling in cardiac myocytes has been observed. To understand the mechanisms of this impairment, we have studied the effect of experimentally induced myocardial injury on Ca^{2+} release activation at the level of individual release sites.

Material and Methods: Single subcutaneous injection of 150 mg/kg isoproterenol (ISO) was used to induce myocardial injury (MI) in rats [1]. The MI model resulted in left ventricular hypertrophy accompanied by a slightly decreased systolic function two weeks after ISO application [2]. Left ventricular myocytes were isolated and studied using patch clamp and confocal microscopy [3] on day 15 after the ISO injection. Whole cell calcium currents and local Ca^{2+} release events (Ca-spikes) were evoked by step depolarizations from -50 to 0 mV. Ca-spikes were measured using 1 mM Oregon Green 488 BAPTA-5N as the Ca^{2+} indicator and 4 mM EGTA to limit Ca^{2+} diffusion. The amplitude, latency and kinetic parameters of Ca-spikes were analyzed [3] and compared in control and MI myocytes.

Results and Discussion: In MI myocytes, the Ca-spikes occurred later after stimulation and were less synchronized than in control myocytes. The latency and synchrony of Ca-spikes were strongly dependent ($P<0.0001$) on the Ca^{2+} current density in MI, but not in control myocytes. These findings indicate impaired DHPR-RyR communication. The activation rate of Ca^{2+} release in evoked Ca-spikes was lowered by 21.4 % in MI myocytes compared to control. In contrast to the latency and the synchrony of Ca^{2+} release, the activation rate of

Ca-spikes did not correlate with the Ca^{2+} current density, indicating a decrease of RyR activity. This decrease might be a symptom of altered state of RyR channels.

Conclusion: The ISO model of myocardial injury revealed changes in cardiac E-C coupling at the level of both, the activity of RyR channels and DHPR-RyR communication. It ascertained the applicability of the employed methodology of Ca-spike measurement and analysis for studies of calcium signaling malfunction in cardiac pathologies.

Acknowledgement
This work was supported by the EU Contract No. LSHM-CT-2005–018833/EUGeneHeart and by the grants APVV-0139-06 and VEGA 2/0102/08.

References
[1] Grimm et al.: *Cardiovasc Res* 37: 418-421, 1998
[2] Králová et al.: *Physiol Res* 57: S83-S89, 2008
[3] Zahradníková jr. et al.: *J Physiol (Lond)* 578: 677-691, 2007

SHIMADZU

Solutions for Science since 1875

Shimadzu LC-30 *Nexera* – skutočný UFLC systém bez kompromisov

Nexera znaky:

- **Tlakový rozsah až do 130Mpa pri prietoku 3mL/min**
- **Ultrarýchly cyklus nástreku 10 sekúnd**
- **Excelentná opakovateľnosť nástrekov**
- **Prakticky nulová krížna kontaminácia bez preplachu ihly**
- **Teplota v termostate do 150degC, s predohriatím mobilnej fázy**
- **Modulárny koncept**

Pre viac informácií nás kontaktujte cez

www.shimadzu.sk.

LIST OF PARTICIPANTS

Antošová Andrea, RNDr.
Institute of Experimental Physics
Slovak Academy of Sciences
Watsonova 47
040 01 Kosice, Slovakia
e-mail: bellova@saske.sk

Balogová Lucia, Mgr.
Department of Biophysics
Faculty of Science
P.J.Safarik University
Jesenna 5
040 01 Kosice, Slovakia
lucia.balogova@student.upjs.sk

Bánó Gregor, Mgr., PhD.
Department of Biophysics
Faculty of Science
P.J.Safarik University
Jesenna 5
040 01 Kosice, Slovakia
e-mail: gregor.bano@upjs.sk

Bernhardt Ingolf, prof.
Laboratory of Biophysics
Saarland University
Campus, House A2.4
66 123 Saarbruecken, Germany
e-mail: i.bernhardt@mx.uni-saarland.de

Bryndzová Lenka, RNDr.
Department of Biophysics
Faculty of Science
P.J.Safarik University
Jesenna 5
040 01 Kosice, Slovakia
e-mail: lenka.bryndzova@yahoo.com

Buriánková Ľuboslava, RNDr.
Department of Biophysics
Faculty of Science
P.J.Safarik University
Jesenna 5
040 01 Kosice, Slovakia
e-mail: luboslava.buriankova@yahoo.com

Búzová Diana, Mgr.
Department of Biophysics
Faculty of Science
P.J.Safarik University
Jesenna 5
040 01 Kosice, Slovakia
e-mail: diana.buzova@gmail.com

Dancáková Alena, Mgr.
Department of Biophysics
Faculty of Science
P.J.Safarik University
Jesenna 5
040 01 Kosice, Slovakia
e-mail: alena.dancakova@student.upjs.sk

Fabriciová Gabriela, RNDr., PhD.
Department of Biophysics
Faculty of Science
P.J.Safarik University
Jesenna 5
040 01 Kosice, Slovakia
e-mail: gabriela.fabriciova@upjs.sk

Faltinová Andrea, Mgr.
Institute of Molecular Physiol. and Genetics
Slovak Academy of Sciences
Vlarska 5
833 34 Bratislava, Slovakia
e-mail: andrea.faltinova@savba.sk

Fedunová Diana, RNDr., PhD.
Department of Biophysics
Institute of Experimental Physics
Slovak Academy of Sciences
Watsonova 47
040 01 Kosice, Slovakia
e-mail: fedunova@saske.sk

Fischerová Jana, Mgr.
Department of Nuclear Physics and Biophysics
Faculty of Mathematics, Physics and Informatics
Comenius University
Mlynska dolina F1
842 48 Bratislava, Slovakia
e-mail: fischerova@ilc.sk

Gaburjáková Jana, Mgr., PhD.
Institute of Molecular Physiol. and Genetics
Slovak Academy of Sciences
Vlarska 5
833 34 Bratislava, Slovakia,
e-mail: jana.gaburjakova@savba.sk

Gaburjáková Marta, Mgr., PhD.
Institute of Molecular Physiol. and Genetics
Slovak Academy of Sciences
Vlarska 5
833 34 Bratislava, Slovakia,
e-mail: marta.gaburjakova@savba.sk

Garaiová Zuzana, Mgr.
Department of Nuclear Physics and Biophysics
Faculty of Mathematics, Physics and Informatics
Comenius University
Mlynska dolina F1
842 48 Bratislava, Slovakia
e-mail: garaiova.zuzana7@gmail.com

Gažová Zuzana, RNDr., CSc.
Department of Biophysics
Institute of Experimental Physics
Slovak Academy of Sciences
Watsonova 47
040 01 Kosice, Slovakia
e-mail: gazova@saske.sk

Hianik Tibor, prof., RNDr., DrSc.
Department of Nuclear Physics and Biophysics
Faculty of Mathematics, Physics and Informatics
Comenius University
Mlynska dolina F1
842 48 Bratislava, Slovakia
e-mail: tibor.hianik@fmph.uniba.sk

Huntošová Veronika, RNDr.
Department of Biophysics
Faculty of Science
P.J.Safarik University
Jesenna 5
040 01 Kosice, Slovakia
e-mail: veronika.huntosova@upjs.sk

Janíček Radoslav, Mgr.
Institute of Molecular Physiol. and Genetics
Slovak Academy of Sciences
Vlarska 5
833 34 Bratislava, Slovakia,
e-mail: radoslav.janicek@savba.sk

Kada Gerald, Dr.
Agilent Technologies
Aubrunnerweg 11
4040 Linz, Austria
e-mail: Gerald_kada@agilent.com

Kaljarová Daniela, Mgr.
Department of Nuclear Physics and Biophysics
Faculty of Mathematics, Physics and Informatics
Comenius University
Mlynska dolina F1
842 48 Bratislava, Slovakia
e-mail: danisssima@gmail.com

Karlovská Janka, Mgr., PhD.
Faculty of Pharmacy
Comenius University
Odbojarov 10
832 32 Bratislava, Slovakia
e-mail: karlovska@fpharm.uniba.sk

Klacsová Mária, Mgr.
Department of Nuclear Physics and Biophysics
Faculty of Mathematics, Physics and Informatics
Comenius University
Mlynska dolina F1
842 48 Bratislava, Slovakia
e-mail: klacsova@fpharm.uniba.sk

Krafčík Andrej, RNDr.
Department of Nuclear Physics and Biophysics
Faculty of Mathematics, Physics and Informatics
Comenius University
Mlynska dolina F1
842 48 Bratislava, Slovakia
e-mail: andrej.krafcik@gmail.com

Lacinová Ľubica, RNDr., DrSc.
Institute of Molecular Physiol. and Genetics
Slovak Academy of Sciences
Vlarska 5
833 34 Bratislava, Slovakia
e-mail: lubica.lacinova@savba.sk

Miškovský Pavol, prof. RNDr., DrSc.
Department of Biophysics
Faculty of Science
P.J.Safarik University
Jesenna 5
040 01 Kosice, Slovakia
e-mail: pavol.miskovsky@upjs.sk

Muššáková Erika, RNDr.
Department of Biophysics
Faculty of Science
P.J.Safarik University
Jesenna 5
040 01 Kosice, Slovakia
e-mail: ardilla@centrum.sk

Novotová Marta, RNDr., CSc.
Institute of Molecular Physiol. and Genetics
Slovak Academy of Sciences
Vlarska 5
833 34 Bratislava, Slovakia
e-mail: marta.novotova@savba.sk

Omar Moktar Amhmed, RNDr.
Department of Biophysics
Faculty of Science
P.J.Safarik University
Jesenna 5
040 01 Kosice, Slovakia
e-mail: Omar1676@gmail.com

Ondriaš Karol, RNDr., DrSc.
Institute of Molecular Physiol. and Genetics
Slovak Academy of Sciences
Vlarska 5
833 34 Bratislava, Slovakia
e-mail: karol.ondrias@savba.sk

Parnica Jozef, Mgr.
Department of Biochemistry
Faculty of Science
P.J.Safarik University
Moyzesova 11
040 01 Kosice, Slovakia
e-mail: jozef.parnica@gmail.com

Pullmannová Petra, Mgr.
Department of Physical Chemistry
Faculty of Pharmacy
Comenius University
Odbojarov 10
832 32 Bratislava, Slovakia
e-mail: petrapullmannova@gmail.com

Rusnák Andrej, Ing.
Institute of Molecular Physiol. and Genetics
Slovak Academy of Sciences
Vlarska 5
833 34 Bratislava, Slovakia,
e-mail: andrej.rusnak@savba.sk

Martin Savko, RNDr., PhD.
Department of Biophysics
Faculty of Science
P.J.Safarik University
Jesenna 5
040 01 Kosice, Slovakia
e-mail: martin.savko@upjs.sk

Staničová Jana, doc., RNDr., PhD.
Department of Biophysics and
Biomathematics
University of Veterinary Medicine and
Pharmacy in Kosice
Komenskeho 73
041 81 Kosice, Slovakia
e-mail: stanicova@uvm.sk

Suchánek Jaromír, RNDr., PhD.
Department of Informatics
A. Dubcek University of Trencín
Pri Parku 19
911 06 Trencín, Slovakia
e-mail: hisym@mail.t-com.sk

Šimšíková Michaela, Mgr.
Department of Biochemistry
Faculty of Science
P.J.Safarik University
Moyzesova 11
040 01 Kosice, Slovakia
e-mail: michaela.simsikova@gmail.com

Šipošová Katarína, Mgr.
Department of Biochemistry
Faculty of Science
P.J.Safarik University
Moyzesova 11
040 01 Kosice, Slovakia
e-mail: katkasiposova@gmail.com

Štroffeková Katarína, RNDr., CSc.
Department of Biophysics
Faculty of Science
University of P.J.Safarik
Jesenna 5
040 01 Kosice, Slovakia
e-mail: katarina.stroffekova@upjs.sk

Tencerová Barbora, Mgr.
Institute of Molecular Physiol. and Genetics
Slovak Academy of Sciences
Vlarska 5
833 34 Bratislava, Slovakia,
e-mail: barbora.tencerova@savba.sk

Tokár Tomáš, RNDr.
Department of Biophysics
Faculty of Science
P.J.Safarik University
Jesenna 5
040 01 Kosice, Slovakia
e-mail: tomastokar@gmail.com

Tomášková Zuzana, Mgr., PhD.
Institute of Molecular Physiol. and Genetics
Slovak Academy of Sciences
Vlarska 5
833 34 Bratislava, Slovakia,
e-mail: zuzana.tomaskova@savba.sk

Topor Peter, RNDr.
Department of Nuclear Physics and Biophysics
Faculty of Mathematics, Physics and Informatics
Comenius University
Mlynska dolina F1
842 48 Bratislava, Slovakia
e-mail: peter.topor@fmph.uniba.sk

Uličný Jozef, doc., RNDr., CSc.
Department of Biophysics
Faculty of Science
P.J.Safarik University
Jesenna 5
040 01 Kosice, Slovakia
e-mail: jozef.ulicny@upjs.sk

Zahradník Ivan, RNDr., CSc.
Institute of Molecular Physiol. and Genetics
Slovak Academy of Sciences
Vlarska 5
833 34 Bratislava, Slovakia,
e-mail: ivan.zahradník@savba.sk

Zahradníková Alexandra, Ing., CSc.
Institute of Molecular Physiol. and Genetics
Slovak Academy of Sciences
Vlarska 5
833 34 Bratislava, Slovakia,
e-mail: alexandra.zahradnikova@savba.sk

Zahradníková Alexandra, jr. RNDr., PhD.
Institute of Molecular Physiol. and Genetics
Slovak Academy of Sciences
Vlarska 5
833 34 Bratislava, Slovakia,
e-mail: saschia.zahradnikova@savba.sk

AUTHOR INDEX